LIGNIN AS AN ANTISTATIC ADDITIVE FOR COMMON POLYMERS

A THESIS SUBMITTED TO

THE GRADUATE SCHOOL OF ENGINEERING AND SCIENCE

OF BILKENT UNIVERSITY

IN PARTIAL FULFILLMENT OF THE REQUIREMENTS FOR

THE DEGREE OF

MASTER OF SCIENCE

IN

CHEMISTRY

By

Tutku BEDÜK

January 2018

LIGNIN AS AN ANTISTATIC ADDITIVE FOR COMMON POLYMERS

By Tutku BEDÜK

January 2018

We certify that we have read this thesis and that in our opinion it is fully adequate, in scope and in quality, as a thesis for the degree of Master of Science.

_____

Bilge BAYTEKİN (Advisor)

_____

Engin Umut AKKAYA

_____

Ali ÇIRPAN

Approved for the Graduate School of Engineering and Science:

_____

Ezhan KARAŞAN

Director of the Graduate School

ABSTRACT

LIGNIN AS AN ANTISTATIC ADDITIVE FOR COMMON POLYMERS

Tutku BEDÜK

M.S. in Chemistry

Advisor: Bilge BAYTEKİN

January 2018

Static electricity is a common phenomenon that can causes million-dollar loses in industries such as polymer, air and space, and drug manufacture due to the detrimental effects of electrostatic discharge of the accumulated charges on surfaces. Doping of the materials, i.e. polymers, with antistatic agents can reduce or prevent these problems. So far, the antistatic additives used were chosen to make the final material/composite conductive to dissipate the surface charges, by either directly doping with conductive materials (e.g. metals or carbon powder), or by doping with additives (e.g. ions) to increase surface humidity. The doped materials usually lose their inherent properties such as the mechanical properties because of the high concentrations of the additive. To provide a more universal solution to this problem and avoid the changes in the material properties after doping, the mechanism of static charge formation, which has been on debate for many years, should be clarified. Recent studies of our group and others have shown that the main mechanism behind the charge formation on electrified (polymer) materials is the bond-breakages on the surfaces of the materials, which lead to mechanoanion, mechanocation, mechanoradical active ends. The former two accounts for the charge on the surfaces and, as we have shown, the latter group (mechanoradicals) stabilizes the charged species. Previously, in our group, it was shown that by removing the mechanoradicals with radical scavenger antioxidants one can destabilize the charges – doping with antioxidants makes materials antistatic. However, the scavenger antioxidants we had used in this example to show the antistatic behavior were far from being practical in use for general polymers -that are produces in millions of tons per year- because of their individual prices. Lignin is the world's second most abundant polymer. It has antioxidant properties, so it is a good candidate as an

antistatic agent for common polymers. In this study we assess the lignin's antistatic action by doping it into common polymers - elastomers (silicon rubber) and thermoplastics (PE, PP, PVC), and comparing the accumulated net charge on the doped and undoped polymers upon contact electrification. It was shown that the increase in lignin concentration and decrease in particle size of the lignin enhances the antistatic property in the polymers, due to an increase in radical scavenging OH groups, as verified by ^{31}P-NMR analysis. We certify that the antistatic property is because of the radical scavenging action and not by increase in the surface conductivity. By doping polymers with cheap and abundant lignin, we provide a more universal, environment-friendly method for preventing electrostatic charge accumulation on common polymers, which are produced in millions of tons per year.

Keywords: *antistatic, polymer, lignin, static electricity, mechanoradicals, mechanochemisty, cryomilling, ultrasonication*

ÖZET

POLİMERLER İÇİN ANTİSTATİK KATKI MALZEMESİ OLARAK LİGNİN

Tutku BEDÜK

Kimya, Yüksek Lisans

Tez Danışmanı: Bilge BAYTEKİN

Ocak 2018

Statik elektriklenme ve yüzeylerde biriken yüklerin zararlı etkileri nedeniyle polimer, hava ve uzay, ilaç üretimi gibi endüstrilerde milyonlarca dolar zarara neden olan yaygın bir sorundur. Malzemelerin ya da polimerlerin, antistatik katkı malzemeleriyle katkılanması, bu problemi azaltabilir veya önleyebilir. Şimdiye kadar, kullanılan ürünü doğrudan iletken hale getiren antistatik katkı maddeleri, yüzeyde oluşan yükleri dağıtmak için kullanılıyordu. Bu malzemeler ürünü / kompoziti; doğrudan iletken yapabilen, metal ya da karbon tozu gibi malzemelerdir. Bir diğer yöntem ise; yüzey nemini artıran katkı malzemeleri (iyonlar gibi) kullanarak yüzey yüklerini azaltmaktır. Fakat katkılama yapılan malzemeler genellikle katkı maddelerinin yüksek konsantrasyonları sebebiyle doğal özelliklerini (ör. mekanik özellikler gibi) kaybederler. Bu soruna daha evrensel bir çözüm sağlamak ve katkılama sonrası malzemenin doğal özelliklerinde meydana gelen değişiklikleri önlemek için, uzun yıllardır tartışılan statik yük oluşum mekanizması açıklığa kavuşturulmalıdır. Son zamanlarda mekanizma üzerinde yapılan çalışmalar, elektrik ile yüklenen malzemeler üzerindeki yük oluşumunun arkasındaki ana mekanizmanın, yüzeylerde bağ kırılması sebebi ile, mekanoanyon, mekanokatyon, mekanoradikal aktif uçlarının oluştuğunu göstermektedir. Mekanokatyon ve mekanoanyonlar yüzeydeki yüklenmeye sebep olurken, mekanoradikaller ise yüzeydeki bu yüklenmenin sabitlenmesini sağlar. Buradan yola çıkılarak daha sonra, katkı malzemesi olarak radikal tuzaklayıcı antioksidanlar ile mekanoradikallerin ortamdan uzaklaştırılması ve yüzeydeki yüklenmenin azaltılması sağlanabilmiştir. Bu yöntem ile polimer malzemenin diğer özellikleri (elektrik ve mekanik özellikler)

korunarak malzemeye antistatik özellik kazandırılabilmiştir. Fakat yine de kullanılan tuzaklayıcıların maliyeti nedeniyle bu yeni yöntem endüstriye uygulanamamaktadır.

Bu çalışmada, genel kullanım polimerlerine antistatik özelliği kazandırmak için kullandığımız radikal tuzaklayıcı antioksidan madde, uygun fiyatı, yılda milyonlarca ton üretimi ve genel polimerler için pratik kullanımı ile yukarıda anlatılan yöntemi uygulamada da pratik hale getirecek *lignin*dir. Lignin dünyada en yaygın olarak bulunan ikinci polimerdir. Antioksidan özelliklere sahip olduğundan, yaygın polimerler için antistatik bir katkılama maddesi olarak iyi bir adaydır. Çalışmamızda, genel kullanım polimerlerinin iki türü olan elastomer (silikon kauçuğu) ve termoplastik (PE, PP, PVC) içine (fındık kabuğundan izole edilmiş) lignin katkılanıp, ligninin polimerlere antistatik özelliği kazandırdığı dokunma elektriklenmesi ile elektriklenmiş polimerlerin net yük ölçümleriyle gösterilmektedir. Bu ölçümlere göre ligninin konsantrasyonu artırıldığında ya da parçacık büyüklüğü azaltıldığında, yani radikal tuzaklayıcısı lignin grupları olan OH grupları artırıldığında (bu artış, ^{31}P-NMR ile kanıtlanmaktadır), polimerler daha az elektrik yükü barındırabilmektedirler. Lignin katkılanan polimerlerin göstermekte olduğu bu antistatik özelliğin radikal tuzaklayıcı mekanizma ile olduğu ve polimerin iletkenliğinin artmasından dolayı olmadığı da çalışmada gösterilmiştir. Sonuç olarak, polimerleri ucuz ve kolaylıkla elde edilebilen lignin ile katkılayarak, yılda milyonlarca ton üretilen, genel kullanım polimerleri üzerinde elektrostatik yük birikiminin önlenmesi için daha evrensel, çevre dostu bir yöntem sunmaktayız.

Anahtar sözcükler: *antistatik, polimer, lignin, statik elektrik, mekanoradikaller, mekanokimya, soğuk öğütme, ultrasonikasyon*

Acknowledgements

This work could not have been carried out without valuable help of my advisor Assist. Prof. Bilge Baytekin. I want to thank her for giving me her guidance, support and motivation always when I needed. I also thank former and present members of this research group. They provided me valuable help during research time.

Beyond this, I am thankful to the examining committee members, Prof. Engin Umut Akkaya and Prof. Ali Çırpan, for their time and help. I would also like to acknowledgement TÜBİTAK for the financial support under project no: **116Z523.**

Also, I want to thank my dearest friends Muammer Yaman and Merve Balci for their endless support and help.

Last but not the least, I would like to thank my husband Timur Ashirov not only for endless support, love and care but also for his great ideas and help during my studies. Furthermore, I am grateful to my parents Oya, and Ilhan Bedük, and my sister Duygu Beduk for their unlimited support, love and encouragement throughout my life and all my studies.

.

TABLE OF CONTENTS

1 INTRODUCTION 1
1.1 Lignin 1
1.1.1 General Information 1
1.1.2 Sources 3
1.1.3 Structure and Chemical Properties 5
1.1.4 Mechanical and Thermal Properties 9
1.1.5 Reactivity 10
1.1.6 Applications 10
1.1.7 The Structure of Hazelnut Shell 11
1.2 Contact Electrification 12
1.2.1 General information 12
1.2.2 Antistatic property 13
1.2.3 The Aim of Thesis 14
2 EXPERIMENTAL 16
2.1 Materials 16
2.1.1 Extraction of Lignin 16
2.1.2 Production of Nano and Micro Lignin 17
2.1.3 Doping Polymers with Lignin 19
2.1.4 Surface Charge Density Measurements 20
2.2 Instrumentation 22
2.2.1 Cryomill 22
2.2.2 Ultrasonication Probe 22
2.2.3 Electrometer 22
2.2.4 Zeta Sizer 22
2.2.5 Fourier Transform Infrared Attenuated Total Reflectance (ATR) 22
2.2.6 Scanning Electron Microscopy (SEM) 22
2.2.7 ^{31}P NMR Analysis 23
2.2.8 UV-Vis Spectrometer Analysis 23
2.2.9 Semiconductor Parameter Analyzer & Probe Stations 23

3 RESULTS & DISCUSSION 24
3.1 Characterization of Extracted Lignin 24
3.1.1 FTIR-ATR Spectroscopy Analysis 24
3.1.2 Scanning Electron Microscopy (SEM) Analysis 28
3.1.3 ^{31}P NMR Spectroscopy 30
3.1.4 UV-VIS Spectrometry 32
3.2 Particles Size Measurements 33
3.2.1 Particle Size of Extracted Lignin 33
3.2.2 Particle Size of Cryomilled Lignin 33
3.2.3 Particle Size of Ultrasonicated Lignin 36
3.3 Electrostatic Measurements 39
3.3.1 Contact charging of Nutshell doped PDMS 40
3.3.2 Contact Charging of Extracted Lignin and Alkali Lignin Doped PDMS 41
3.3.3 Contact Charging of Cryomilled and Ultrasonicated Lignin Doped PDMS 43
3.3.4 Contact Charging of Extracted Lignin with Different Concentrations Doped PDMS 44
3.3.5 Contact Charging of Extracted Lignin Doped Thermoplastics 45
3.4 Resistivity Measurements 48
4 CONCLUSION 49
5 BIBLIOGRAPHY 1

LIST OF FIGURES

Figure 1: Lignin content in secondary cell wall 2
Figure 2: Different lignin types and utilization methods 4
Figure 3: General chemical structure of lignin 5
Figure 4: Generic lignin units 6
Figure 5: Three monomers of lignin structure 6
Figure 6: Common functional groups of lignin structure [12]. 7
Figure 7: The main types of linkages of lignin structure [14, 15]..... 8
Figure 8: Hazelnut shell [13]..... 11
Figure 9. Traditional (conventional) methods for prevention of electrostatic discharge versus the new approach based on the mechanism of charge formation and stabilization in polymers (left). Surface resistivity threshold and ranges for conductivity and antistatic behavior. Antistatic behavior is obtained with surface resistivity values above 10^{10} Ohm/sq. 14
Figure 10. a) Cryomilling instrument (from www.retsch.com), b) Ultrasonication horn (from www.hielscher.com) 18
Figure 11. PDMS only, lignin solution doped PDMS pieces with different concentrations and solid lignin doped PDMS pieces. 19
Figure 12. Different lignin solutions with the concentrations of 0.014, 0.020, 0.028, 0.034 and 0.040 mg/ml, increasing from 5 to 1..... 20
Figure 13. Schematic representation of experiment procedure..... 21
Figure 14. FTIR spectrum of lignin from 26
Figure 15. a) FTIR spectra of lignin monitoring increasing cryomilling time. b) Magnified O-H stretching region, c) Aromatic and skeletal vibrations region. 27

Figure 16. ATR spectrum of the lignin after acid-extraction from the nut shell (red line) and ATR spectrum of this extracted lignin after cryomilling and subsequent ultrasonication (‘nanolignin’, black line). 28
Figure 17. SEM images of alkali lignin particles: a-c) before and d-f) after mechanochemical treatment. 29
Figure 18. SEM images of extracted lignin particles (see experimental part for acid-extracted lignin): a-c) before and d-f) after mechanochemical treatment involving first cryomilling of 100 mg sample for 60 min, then 30 mg of the cryomilled sample sonicated for 60 min at 20 kHz. 30
Figure 19. ^{31}P NMR spectra of extracted lignin milled between 0-120 mins. 31
Figure 20. ^{31}P NMR spectra of lignin before and after milling, taken from the literature 31
Figure 21. .UV-VIS spectra of acid-extracted lignin (see experimental) solutions at the concentrations of concentrations of 0.040, 0,034, 0.028, 0.020, 0.014 mg/ml. The intensity of peak with absorption maximum at 241 nm is increasing with increasing concentration. 32
Figure 22. ZetaSizer data for different cryomilling times: a) 0 b) 5 c) 10 and d) 20 mins. 34
Figure 23. ZetaSizer data for different cryomilling times: a) 30 b) 40 c) 60 and d) 120 mins. 35
Figure 24. ZetaSizer data for different ultrasonication times: a) 5 b) 10 c) 20 and d) 30 mins. 37
Figure 25. ZetaSizer data for different ultrasonication times: a) 40 b) 60 and c) 120 mins. 38
Figure 26. a) Particle size vs cryomilling times and b) Particle size vs ultrasonication times. 39
Figure 27: Contact charge accumulated on PDMS pieces doped with ground nutshell and undoped PDMS pieces (1 cm x 1 cm x 0.6 cm) with respect to the number of touches to Al sheet. 60 mg nutshell was milled for 20 minutes by Cryomill and directly doped into PDMS. 41
Figure 28. Contact charge accumulated on PDMS pieces doped with ‘protonated’ alkali lignin and acid-extracted lignin from nutshell, and undoped PDMS pieces (1 cm x 1 cm x 0.6 cm) with respect to the number of touches to Al sheet. 30 mg of lignin with the same particle size (101.2±2.1 nm) was used

to dope PDMS. Protonated alkali lignin is prepared as follows: 20 mL solution by addition of 1.0 g alkali lignin was dissolved in 20 mL water, then this solution was titrated with 20 ml HCl solution prepared by dilution of 1.6 ml 37% HCl. The precipitate formed was filtered and dried. 42

Figure 29. Contact charge accumulated on PDMS pieces doped with lignin solution having 1000±2.1, 543.4±2.5, 357.6±3.2, 147.8±3.0, 101.2±2.1 and 24.04±3.5 nm, lignin particles, and undoped PDMS pieces (1 cm x 1 cm x 0.6 cm) with respect to the number of touches to Al sheet. Charge of lignin solution doped PDMS pieces decreases with decreasing particle size of lignin in the solution. 43

Figure 30. Contact charge accumulated on PDMS pieces doped with lignin solution having 0.04 mg/ml, 0.034 mg/ml, 0.028 mg/ml, 0.020 mg/ml, and 0.014 mg/ml lignin concentrations, and undoped PDMS pieces (1 cm x 1 cm x 0.6 cm) with respect to the number of touches to Al sheet. Particle size = 101.2±2.1 nm. As the concentration of lignin in the solution and thus in the final composite increases, PDMS acquires less charge. 44

Figure 31. a) Decay curves of lignin solution doped PDMS pieces lignin having particle size of 1000±2.1, 543.4±2.5, 357.6±3.2, 147.8±3.0, 101.2±2.1 and 24.04±3.5 nm. b) Decay curves of lignin solution doped PDMS pieces with lignin concentration of 0.04 mg/ml, 0.034 mg/ml, 0.028 mg/ml, 0.020 mg/ml, and 0.014 mg/ml 45

Figure 32. PP doped with lignin reduces charging and adhesion to pieces of paper after contacting with a piece of nylon for 500 times. A piece of a) undoped PP, b) PP doped with lignin was brought close to small pieces of paper. . 46

Figure 33. Charging curves of a)lignin doped PP and PP only, b)lignin doped PE and PE only, c)lignin doped PVC and PVC only. Polymers were doped with 60 mg of lignin. The charge of polymers decreases as a result of doping solid lignin into the PDMS pieces. 47

Figure 34. I-V curves of a) lignin doped polypropylene. and b) undoped polypropylene. Samples are 20 mm wide and distance between electrodes is 100 µm. 48

LIST OF TABLES

Table 1: Average cellulose, hemicellulose, lignin compositions of several lignocellulosics 3
Table 2: Some characteristics of different types of industrial lignins 5
Table 3**:** Elemental analysis of nutshell [26]..... 11
Table 4: Compositions of nutshell in terms of cellulosic and lignin components [26]. 12
Table 5. FTIR vibration frequencies detected in ATR spectrum of acid-extracted lignin (see experimental part) and the corresponding peak assignments from groups 25

CHAPTER 1

1 INTRODUCTION

1.1 Lignin

1.1.1 General Information

Lignin is an organic polymer that binds fibers, veins and cells together in plants. Lignin composition of the wood stems is between 15% and 40% [1]. Wood consists of three main macromolecular species: cellulose, hemicellulose, and lignin. There are also minor components in wood such as pectin, fats, wax, and moisture.

Lignin is one of the main components of a cell wall in all vascular plants and in the woody stems of hardwood and softwoods plants. It provides tree with unique strength and elastic properties. The superior mechanical properties of wood are directly related to lignin [1-5]. Primitive plants such as fungi and algae, which do not have differentiated cell tissues, do not contain lignin. The secondary cell wall in the cell is the part that stores the lignin. This cell wall has large tissue volume and large storage capacity for lignin molecule (Figure 1). Extraction methods of lignin generally includes passing through the secondary cell wall for the diffusion of the lignin. Lignin has an important role as water sealant in the stems. Also, it helps to control water transport through the cell wall and to protect plants against biological attack by hampering enzyme penetration. Other than giving strength to the plant, lignin also maintains fluid flow and protects woody plants against the chemical or biological attacks [6]

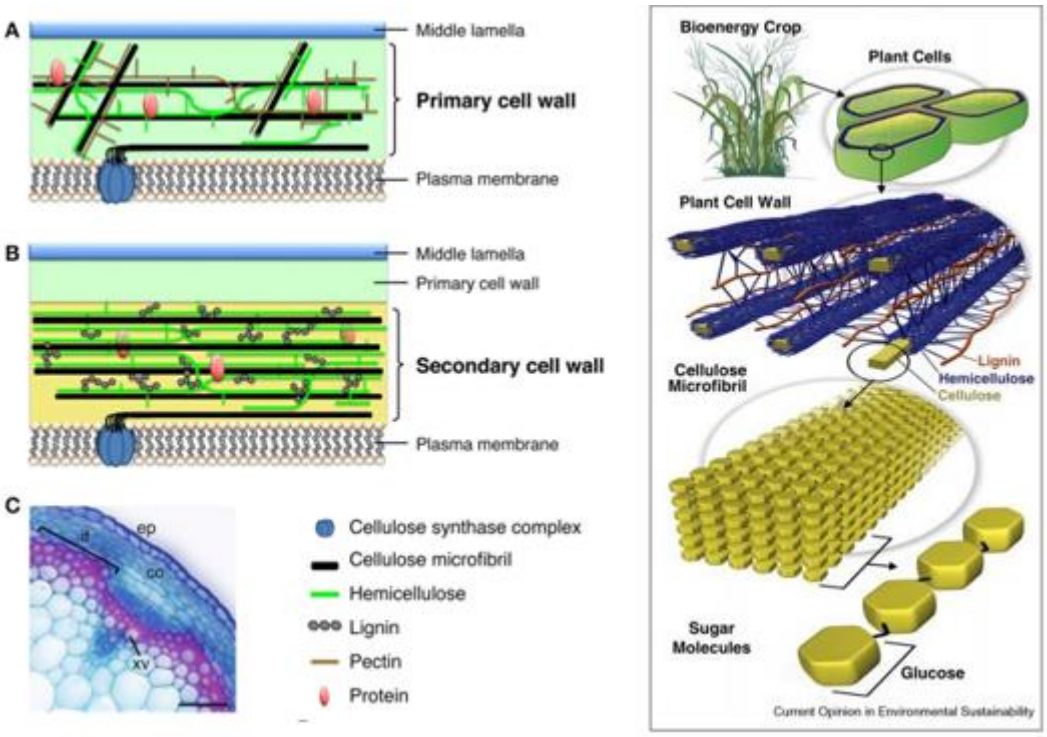

Figure 1: Lignin content in secondary cell wall [7].

Another importance of lignin is a permanent glue that can bond cells together in the woody stems. As a result of that property, the stems become rigid and impact resistant. The cellulose-hemicellulose-lignin content of lignocellulosic materials inside of wood is shown in Table 2 [1-3]**.** These numbers do not include minor components of lignocellulosic materials. Lignin content can be seen for hardwood and softwood plants.

Species	Type	Cellulose	Hemicellulose	Lignin
White spruce	Softwood	44	29	27.1
Eastern hemlock	Softwood	42	32.5	26
Eastern white cedar	Softwood	41	26	31
American elm				
White birch	Hardwood	51	23	24
Flax	Hardwood	42	38	19
Jute	Bast Fiber	75.9	20.7	3.4
Hemp	Bast Fiber	84	15.7	0.3
Coir	Bast Fiber	79.9	19.2	0.9
	Seed Fiber	46.7-48.7	0.2-0.3	51-53

Table 1: Average cellulose, hemicellulose, lignin compositions of several lignocellulosics [8].

Discovery of Lignin

Anselme Payen discovered cellulose and its abundance of all the plants and their cell walls, in 1838. He also isolated cellulose for the first time in the history. Not only he discovered cellulose, he also tried to separate wood into its component parts and isolated lignin from wood by treating wood with nitric acid and alkaline solutions. Payen named the compound that he found as 'incrustant'. Later, in 1857, this compound was named as 'lignin' by German scientist Shulze. At that time, the general definition of the lignin was described as " *Polymeric natural products arising from an enzyme initiated dehydrogenative polymerization of three primary precursors: transconiferyl, trans-sinapyl, and trans-p-coumaryl.*" [8].

1.1.2 Sources

The lignin composition of plants alters according to species and the environment that the species are present. Woody plants have the largest lignin concentrations – lignin is mostly present in their stems.

Lignin is a name given to a broad set of polymers, which have same monomers (see below) but with different connectivities. Different lignin species can exist at the same plant. The lignin in the cell wall is always present with hemicelluloses. There are

both non-covalent and covalent bonds in all lignin types. Many lignin types contain aromatic carboxylic acids in the esterified state and the chemical composition of the lignin types may change. In general, they can be defined as branched polymers of phenyl propene base units.

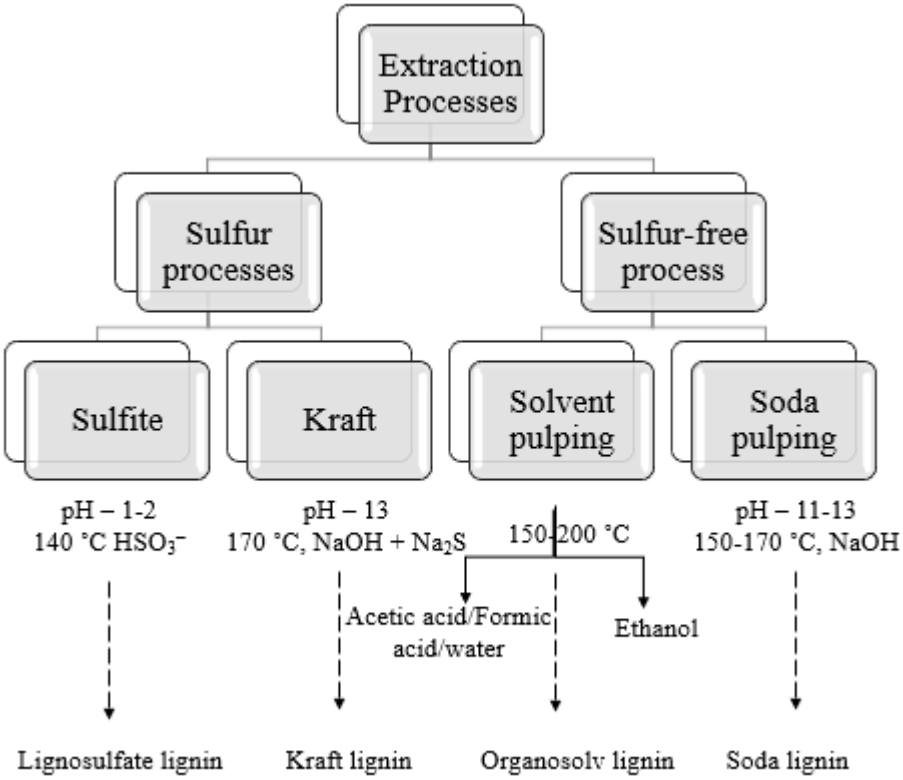

Figure 2: Different lignin types and utilization methods [9].

Lignin is categorized as sulfur and non-sulfur lignin according to different extraction processes (Figure 2). Commercially available lignin type is the product of Sulfur containing process. There are two types of products of Sulfur containing extraction process, lignosulfonates and Kraft lignin [10]. In the second method of extraction sulfur is not used and sulfur-free lignin is obtained. However, this process is not yet commercially viable. Organosolv and Soda lignin are the two types of products resulted from such Sulfur free extraction process. Physical properties of these lignin types are shown in Table 2 [11].

Lignin type	Sulfur-lignins		Sulfur-free lignins	
	Kraft	Lignosulfonate	Soda	Organosolv
Aspect				
Raw materials	Softwood Hardwood	Softwood Hardwood	Annual plants	Softwood Hardwood Annual plants
Solubility	Alkali Organic solvents	Water	Alkali	Wide range of organic solvents
Number-average molar mass (M_n – g mol^{-1})	1000–3000	15,000–50,000	800–3000	500–5000
Polydispersity	2.5–3.5	6–8	2.5–3.5	1.5–2.5
T_g (°C)	140–150	130	140	90–110

Table 2: Some characteristics of different types of industrial lignins [12].

1.1.3 Structure and Chemical Properties

The chemical structure of lignin is not exactly known due challenges related to 1) the complex nature of the lignin polymers arising from different connectivities of the monomers, 2) to the variety of lignin sources and species. Only a general structure of lignin is attributed to the molecule, which shows a polyphenol (Figure 3). Lignin stability and resistivity against degradation is due to many covalent bonds in the structure as well as some strong non-covalent interactions such as hydrogen bonding [5].

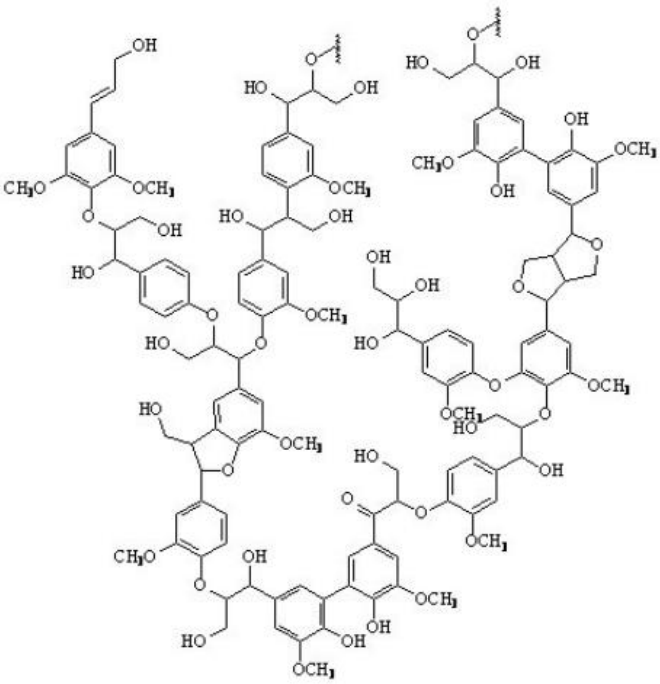

Figure 3: General chemical structure of lignin

Batches of lignin produced in industry and the lignin naturally present may have different structures from each other. [4]. The main difference between these three structural components is the number of methoxy groups (-OCH_3) present attached to the aromatic ring (Figure 4).

Regardless of the source, all lignins are polymers of 4-hydroxycinnamyl alcohol (p-coumaryl alcohol) or its 3- and/or 3,5-methoxylated derivatives, respectively coniferyl and sinapyl alcohol (Figure 5).

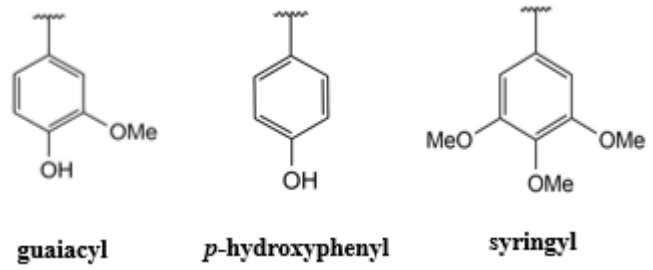

Figure 4: Generic lignin units [13].

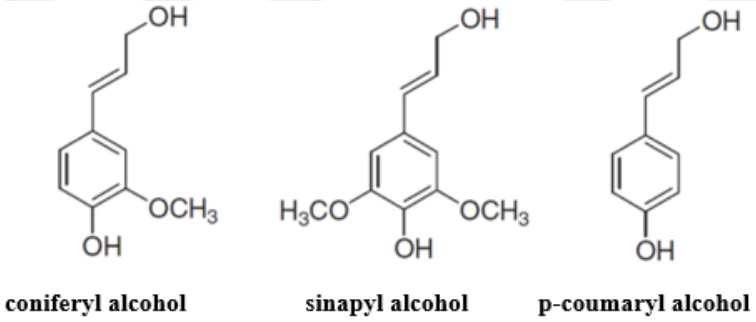

Figure 5: Three monomers of lignin structure

Figure 6 represents the common structural groups of lignin molecule. Biphenyl carbon-carbon linkages between aromatic carbons, alkyl-aryl carbon-carbon linkages between an aliphatic and aromatic carbon, and hydrolysis-resistant ether linkages are the strong linkages of the general lignin structure. On the other hand, the α-aryl ether bonds can hydrolyze, and these bonds are relatively weaker than the other linkages of the structure.

Lignin from similar sources was found to have similar structures and therefore lignin polymers are grouped into 3 classes: softwood, hardwood and grass lignin. As mentioned before, all classes of lignin are based on aromatic monomeric units but they have different attachments. Sjöström and [14] Henriksson [15] stated that 35-70 % of the total linkages belongs to β-O-4' linkages. Softwood lignin is based on guaiacyl- units connected by ether and carbon-carbon linkages. Hardwood lignin consists of approximately equal amounts of guaiacyl- and syringyl- units. Grass lignin has guaiacyl-, syringyl- and p-hydroxyphenyl-propane units in its structure (Figure 4). These three structural groups of lignin are generated from the primary precursors, transconiferyl, trans-sinapyl, and trans-p-coumaryl, which are shown in Figure 5.

Figure 7 indicates the common linkages in the general lignin structure. It is clearly seen that β-O-4-C linkage is more frequently present than the others.

Softwood lignin mostly consists of coniferyl alcohol groups attached to the aromatic rings, On the other hand, hardwood lignin consists of both coniferyl and sinapyl alcohols groups attached to the aromatic rings. Other than softwood and hardwood the grass lignin is stored in grasses and consists of all three alcohols types, coniferyl, sinapyl, and p-coumaryl alcohols attached to the aromatic rings in the structure. The name of ~monolignols~ is used for these three aromatic alcohol groups. The phenolic original forms of these monolignols in the lignin molecule structure are p-hydroxyphenyl, guaiacyl and syringyl groups respectively.

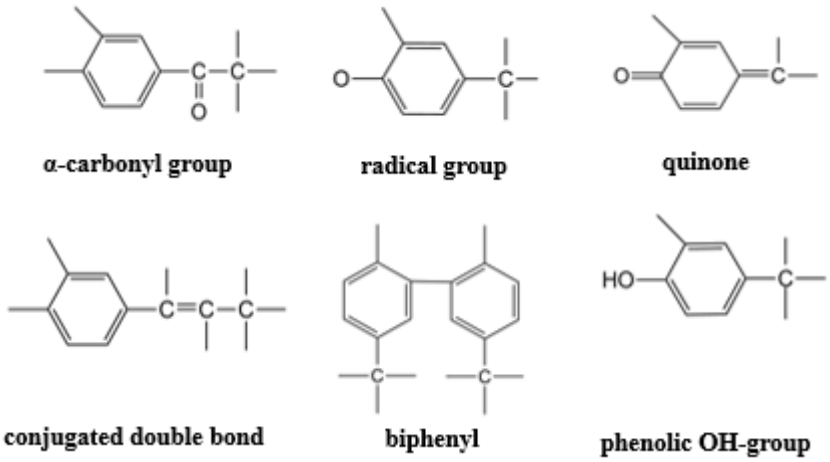

Figure 6: Common functional groups of lignin structure [12].

The percentages of each monomer and their linkages in lignin molecules vary according to the sources of lignin as well as to environmental and cultivating conditions of wood sources.

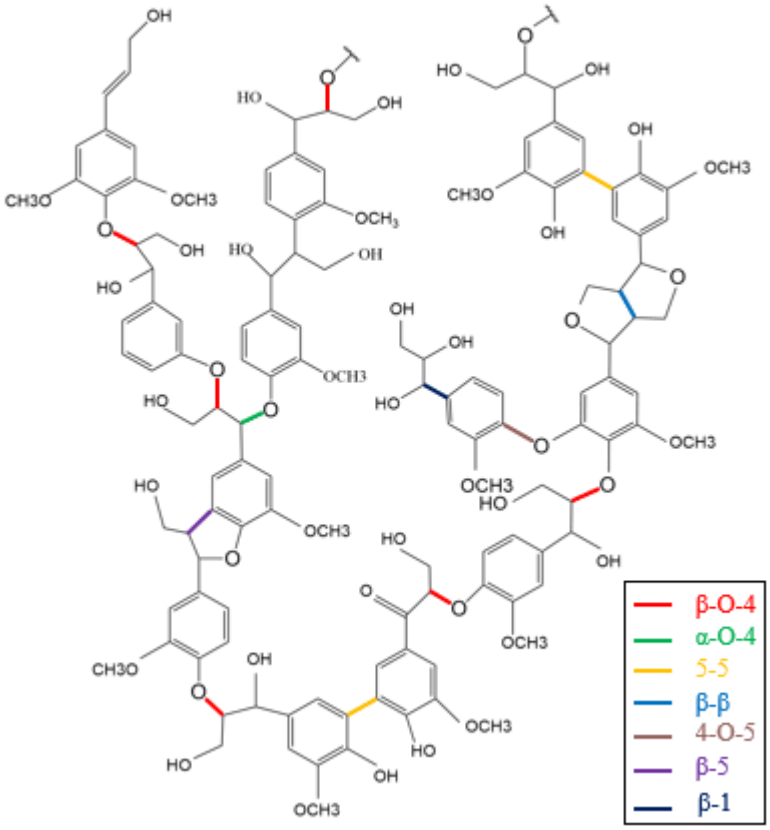

Figure 7: The main types of linkages of lignin structure [7].

As mentioned above, it is not possible to define the exact structure of lignin as a chemical molecule. There is no easy method to determine the structure of lignin and to prove the types of bonding in lignin. In addition to the different ratios of the three monomers, their innumerous ways of getting connected to each other, branching possibilities, the structure of lignin can be even more complicated – some functional groups other than the coniferyl, sinapyl, and p-coumaryl alcohol (bearing different aromatic rings and side chains) can also be encountered in the lignin structure. To our study, the exact chemical structure of lignin is not vitally important, since radical scavenging ability can be supplied by any of the (conjugated) phenols. However, as shown below in the Results and Discussion part, the amount of these functional groups and their availability is important to achieve the antistatic property.

1.1.4 Mechanical and Thermal Properties

Lignin itself is an amorphous polymer and behaves as a thermoplastic material. It has a glass transition temperature Tg, which is dependent on absorbed water, molecular weight, isolation and extraction method.

Decomposition temperature of lignin is a range between 200-600 °C according to the lignin species. The α- and β-O-4' linkages break at the temperature of 150-300 °C [7]. The cleavage between the aliphatic side chains and aromatic ring starts at around 300 °C, while the carbon-carbon bonds between monolignols start to break at the temperature of 370-400 °C. In addition, volatile products such as CO, CO_2, CH_4 and H_2 are formed upon thermal degradation [16]. This range is lower than the degradation temperature of cellulose and the hemicellulose components of biomass of lignin [17]. Decomposition temperatures can be measured by using thermal methods such as differential thermal analysis method (DTA) or thermogravimetric analysis (TGA) [9, 18].

Lignin is a frequently used doping material to alter the mechanical properties of synthetic polymers, especially in thermoplastics [19]. Upon lignin doping, melting temperature of thermoplastics decreases, and polymer's storage modulus increases from 1.24 GPa to 2.25 GPa when lignin was introduced to the polymeric matrix. Doping thermoplastics with lignin leads to a loss of flexibility and increase in strength of the polymer [20, 21].

Doping synthetic polymers with lignin also affects their thermal stability. Thermal analysis studies concluded that lignin doped synthetic polymer composites has enhanced thermal stability than the undoped polymer. The reason of this improvement is the presence of the radical scavenger groups (phenols) in lignin, which renders lignin an antioxidant; the scavenger groups react with the reactive radicals formed during thermal degradation and remove them. We will describe the antistatic property arising from a similar action of these phenolic groups, i.e. their reactions with free radicals, below in the Results and Discussion part.

1.1.5 Reactivity

Lignin's functional groups and their linkages determine the reactivity of lignin. As we show above, there are mainly phenolic hydroxyl and methoxy groups in the general structure and their amounts vary for softwood and hardwood lignin. Methoxy group content in lignin of hardwood plant is greater than the softwood lignin. The reason for that is the high content of sinapyl alcohol groups of lignin in hardwood plants [22].

Each part of the lignin molecule structure influences the reactivity of the molecule differently. Phenolic hydroxyl groups provide the most reactivity among all the functional groups. Only 10-13 % of the aromatic rings are in free phenolic positions as the others form ether bonds [23]. As the size of the lignin is reduced by thermal or mechanical treatment, the number of free phenol groups increases, which is shown to increase the antioxidant of lignin, and hence, the antistatic property of the lignin/polymer composite, as shown below in the Results and Discussion part.

1.1.6 Applications

Cellulose, most abundant polymer in the nature, is obtained from plants. It is the main material used in paper industry [19]. Removing lignin from the woody plants leads to high quality paper with good mechanical properties [18]. More than 70 million tons of lignin is formed as by product of paper pulping industry, which is usually defined as waste. It is possible to buy lignin with different purity percentages for scientific purposes [10]. However, the studies of McCartey at al. showed that the annual sale of produced lignin is the 1% of total lignin production in a single year. The remaining 99% is either disposed or used for the energy recovery step; most of the residual lignin in the forest industry is burned and used as an energy source [24]. Around 95% of industrial lignin is burned due to its good heat value [6, 40]. Lignin, having antioxidant, antibacterial and antiviral properties [9], is a natural and renewable raw material, and its cost is reasonable, it can be used in place of petrochemicals. However, current applications of lignin are limited. Lignin containing products and lignin play an important role in the formation of soil. Lignin is used in food and cosmetic industries to improve properties of emulsions and dispersants [25]. 50-1200 €/ton is the approximate selling price of lignin over the

past decade – this is much lower than common molecular antioxidants such as ascorbic acid, gallic acid, and alpha-tocopherol with prices around 50-100 €/g

1.1.7 The Structure of Hazelnut Shell

Figure 8: Hazelnut shell [13].

Hazelnut shell is a one of the natural source for extraction of lignin. It has one of the highest lignin content (35-50%) among the other sources of lignin. The shell has mainly a wood-like cellulosic structure, consisting of two main layers. Outside layer has a hard structure wrapped with a soft and loose inside layer [26]. The shell is a sensitive material against moisture and water. As surface area increases when the nutshell is crushed, sensitivity against moisture becomes greater. There are not many publications about elemental analysis and content of hazelnut shell. Aşık et al. [27] have studied the elemental analysis and composition of the hazelnut shell (Table 3 and Table 4).

Elemental analysis	**%**
C	45.59
H	4.59
O	38.14

Table 3**:** Elemental analysis of nutshell [27].

	%
Moisture	10.12
Ash	1.26
Oil	1.54
Lignin	37
Cellulose	22.2
Hemicellulose	24.8

Table 4: Compositions of nutshell in terms of cellulosic and lignin components [27].

1.2 Contact Electrification

1.2.1 General information

Static electricity can cause many problems and losses in industries such as polymer, air and space, and drug manufacture. In the pharmaceutical industry, when drug powder interacts with other surfaces, the charge accumulated on the particles may lead to non-uniform blending. Therefore, non-uniform dosage of the products can be formed. Also, electrostatic discharges can cause damages of equipment, and are known to cost the electronic industry billions of dollars per year. Most importantly, these discharges may cause explosion of flammable gases, dusts, and organic liquids. Hence, considering the wide range of undesirable, costly, and dangerous consequences of contact electrification, it is important to develop strategies to prevent the generation of static charge, when solid surfaces come into contact. This is because of the detrimental effects of electrostatic discharge of the accumulated charges on surfaces. Everybody can experience presence of static electricity in daily life [28, 29]. For example, one can easily observe that after rubbing a balloon to someone's hair, balloon sticks to the hair due to static electricity. The concept of contact electrification was first raised about 2500 years ago by Thales. First experiments on contact electrification involved rubbing wool and amber against each other [30], which led to naming of 'electron' after the ancient Greek word for

‘amber’ (at that time, Thales thought minute pieces of amber was transferred to wool upon rubbing).

1.2.2 Antistatic property

In industry, several conventional methods are used to reduce static charge. However, they may cause loses of the mechanical properties of polymeric materials. Additives to increase conductivity directly or through an increase in surface humidity are used in these conventional methods (Figure 9). For the first approach, carbon nano tubes and carbon black, as well as metals are used to promote conductivity for dissipation of static charges [31]. However, these additives can cause losses of the mechanical and physical properties of the polymeric matrix. In the latter approach, the fact that humidity leads to a decrease in charging process on surfaces is used [32]. However, this effect is limited and it possesses are several disadvantages of humidity control. Firstly, humidity control is an expensive method for reduction of static electricity on surfaces. Moreover, increase in surface humidity can also cause corrosion or other adverse side effects. Thus, new and more effective methods are needed to prevent static electricity on the polymeric surfaces [6, 31, 35], and these methods can be developed by taking the new knowledge on mechanism of contact electrification.

A recent previous study has showed that the main mechanism behind the charge formation on electrified materials is the bond-breakages on the surfaces of the polymeric materials, which lead to mechanoanion, mechanocation, mechanoradical active ends [33-35]. It was also shown that mechanocations and mechanoanions coexist on the surface and mechanoradicals stabilize the charged species (mechanoions) [35]. It is possible to destabilize the charges (mechanoions) by removing the mechanoradicals by reacting them with radical scavenger doping materials such as alpha tocopherol (Vitamin E). This new method for obtaining antistatic polymers can be used for common polymers – elastomers and thermoplastics. The method does not involve any conductivity increase of the surface, so the electrical properties of the base material do not change. Moreover, since it does not involve high doping concentrations needed in traditional methods for achieving percolation, the mechanical properties of the base polymer is also retained. However, the new method is not currently applicable to industrial

production since the prices of the molecular antioxidants are high and they are not chemically stability for prolonged use of composites [6, 36-38].

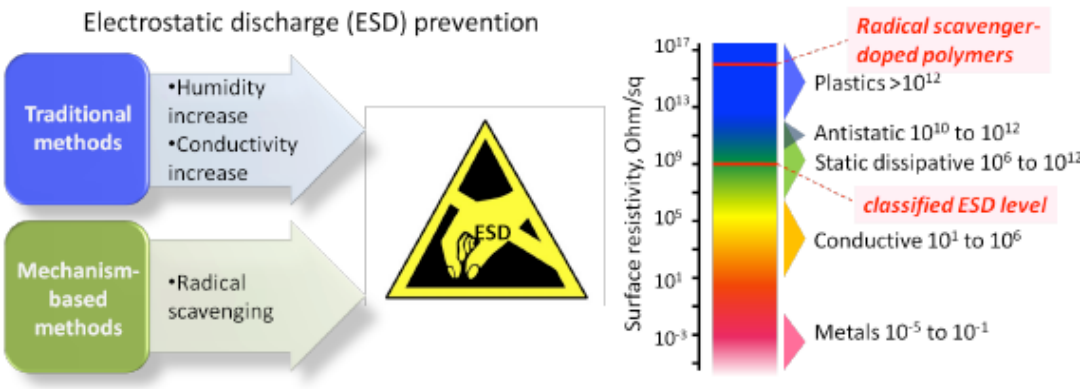

Figure 9. Traditional (conventional) methods for prevention of electrostatic discharge versus the new approach based on the mechanism of charge formation and stabilization in polymers (left). Surface resistivity threshold and ranges for conductivity and antistatic behavior. Antistatic behavior is obtained with surface resistivity values above 10^{10} Ohm/sq.

1.2.3 The Aim of Thesis

In this study, we aim to show that lignin, which is the second most abundant polymer on earth, can be used as a doping material to obtain polymer composites that are resilient against contact charging; i.e. on their surfaces static charges cannot persist. Lignin seems to be a good candidate for such an antistatic doping material because it bears the chemical functional groups that can react with the formed mechanoradicals (which are not charged themselves but stabilize the charges on surfaces) during contact/rubbing event. This reaction can remove the mechanoradicals and destabilize the charges, which is monitored by surface charge density measurements. To increase the number of lignin's phenolic groups in the composite material we 1) increase the concentration of lignin in the polymer composite, 2) decrease the particle size of the doped lignin by cryomilling and ultrasonication. We show the universality of our approach on the choice of the polymeric material by rendering both some examples of elastomers (PDMS) and thermoplastic polymers (PE, PP, and PVC) as polymeric matrix.

We use lignin that was extracted from the nutshell for this study, which is characterized by FTIR spectroscopy and ^{31}P-NMR-spectroscopy. The functional groups of lignin that are critical for the ‘antistatic action’ are identified by FTIR spectroscopy and identification of all types of -OH groups and the content of these groups can be found by ^{31}P-NMR-spectroscopy. We aim to correlate these findings with the above-mentioned surface charge density measurements.

CHAPTER 2

2 EXPERIMENTAL

2.1 Materials

The hazelnut shell used in this study was obtained from Gümeli village in the west black sea region in Turkey. Alkali lignin with low sulfonate content was used as a commercial lignin source and supplied by Sigma Aldrich. Sulfuric Acid 95-97% bought from Sigma Aldrich. 30 ml Autoclave Reactor (PARR Instrument Company) was used in extraction processes of lignin from hazelnut shell. The extracted lignin was separated according to particle sizes by using Retsch Molecular test sieves. Tetrahydrofuran (Merck) was used for Zeta Sizer measurements and 1,4 Dioxane (Carlo Erba) was used to dissolve lignin. Alkali lignin was acidified with Hydrochloric acid 37% (Carlo Erba). For ^{31}P NMR, chromium (III) acetylacetonate (Sigma Aldrich) was used as the relaxation agent. Deuterated chloroform (98%) (Merck KGaA) and extra dry pyridine (99.5%) (Acros) was used for preparation of solvent mixture. Cholesterol (Sigma Aldrich) was used as internal standard for ^{31}P NMR measurements. Lignin samples were derivatized with 2-chloro-4,4,5,5-tetramethyl-1,3,2-dioxaphospholane (Sigma Aldrich). Finally, PDMS pieces were prepared by using Dow Corning Sylgard 184 Silicone Elastomer Kit, using 10:1 ratio of the base to curing agent.

2.2 General Experiment Conditions and Setup

2.1.1 Extraction of Lignin

17-33% of the dry weight of the woody plant generally represents the lignin content of the plant. There are several extraction methods for separation of lignin from woody plants. Compounds of nutshell such as cellulose, hemicellulose, moisture, ash

easily decompose. However, lignin has high resistivity against high temperatures and persists at high temperatures without degradation.

Due to its high content of lignin, nutshell was used as a lignin source. A mortar and a grinder were used to crush nutshells into smaller pieces. At this point, particles were approximately 1 mm. Particle sizes smaller than 100 μm were separated by a 100 μm molecular test sieve. Similarly, particle size smaller than 25 μm were separated by a 25 μm molecular test sieve. Lignin particles with a particle size range between 1 to 25 μm was dried under vacuum at 45 ˚C for 24 hours. These separated particles were used to extract the lignin from nutshell by the acid bomb technique. 5 gr of these nutshell particles was mixed with 10 ml of 72% H_2SO_4 solution (Sigma-Aldrich). (Since the higher acid concentrations may lead to degradation of lignin in the nutshell, 72% H_2SO_4 solution was selected for avoiding the degradation of lignin in the nutshell.) The 'acid bomb' technique was used, by keeping the mixture in an autoclave reactor at 150 °C for 45 minutes. Under these conditions, lignin does not decompose, however, other components of nutshell decompose. After 45 minutes, autoclave reactor was cooled to the room temperature (25 ˚C). (**Be careful!** It is not safe to open the autoclave reactor at high temperatures because the solution mixture of lignin and H_2SO_4 might be boiled up and splash!) After opening the autoclave, the solution mixture of lignin and H_2SO_4 was diluted with 100 ml of distilled water. Mixture was filtered by suction filtration to collect solid lignin. The collected solid lignin was washed with distilled water several times. Finally, collected solid lignin with a pH value of 4, was dried under the vacuum at 30 ˚C. By this method, lignin was extracted from the nutshell.

2.1.2 Production of Nano and Micro Lignin

Sizes of the lignin particles, which are collected after the extraction step may vary due to the aggregation of the lignin particles. Therefore, dried and extracted lignin was crushed with a mortar and pestle for 10 minutes, then 1 to 25 μm size of lignin extracted from nutshell by acid bomb technique was separated from larger lignin particles by 25 μm molecular test sieve (Retsch, Germany), again. At this point, we aimed to further reduce the particle size of extracted lignin to obtain a more homogeneous dispersion of lignin in the composite, to access to a higher number of

phenolic groups in the structure and clarify the relation between the particle size of the lignin and the antistatic property.

To decrease the particle size, we used mechanical methods, which are milling and ultrasonication (Figure 10). Retsch Cryomill instrument was used for milling. Lignin samples were milled with 6 zirconia balls each with 10.06 mm diameter as grinding medium in a zirconia grinding chamber. The extracted solid lignin was milled at 30 Hz frequency for an indicated time (see below) at 77 K (cryo condition). This low temperature is achieved by liquid nitrogen that circulates through the milling chamber. The extracted solid lignin was milled at 30 Hz for 60 minutes. A homogeneous solid lignin was obtained as a result of milling. Particle size of this milled lignin, as analyzed by Zeta Sizer, was found to be 46.3±2.5 nm. We also aimed to identify the effect of different milling durations to the particle size of lignin. The extracted lignin was milled for 5, 10, 20, 30, 40, 60 and 120 minutes. Particle sizes of 959.5±2.3, 724.6±2.5, 679.9±3.2, 686.5±2.1, 543.4±2.5, 461.3±2.1 and 436.7±2.5 nm were obtained respectively.

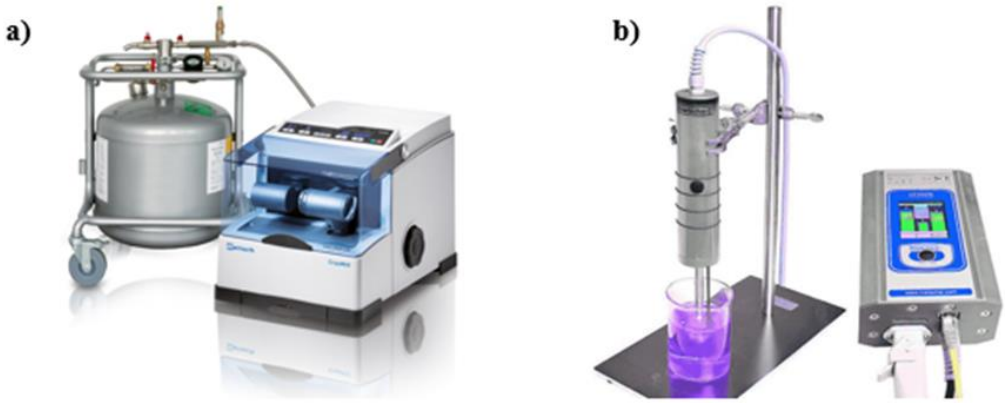

Figure 10. a) Cryomilling instrument (from www.retsch.com), b) Ultrasonication horn (from www.hielscher.com)

Secondly, ultrasonication was used for reducing the particle size of the extracted lignin further. The milled lignin (see above) was suspended in approximately 20 ml of 1,4-Dioxane (Carlo Erba Reagents, Italy). An ultrasonic horn (UP200St Hielscher Ultrasonic Technologies) at 20 kHz frequency, 200 W power was used to sonicate the lignin suspension for 5, 10, 20, 30, 40, 60 and 120 minutes. The sizes of the particles are 402.7±2.8, 357.6±3.2, 260±2.2, 147.8±3.0, 101.2±2.1, 35,45 ±2.4 and

24.04±3.5 nm respectively. Sonication process was performed with 1-minute break for every 5 minutes to prevent overheating of the probe. Schematic representation of the extraction and mechanical treatment procedures can be seen in Figure 13.

2.1.3 Doping Polymers with Lignin

Lignin extracted and size-reduced through the above-described procedures was then doped into polymers. Two types of polymers, elastomer and thermoplastic, were used as the polymeric matrix. The polydimethylsiloxane (PDMS) was chosen because it can be cured to form a smooth surface on flat mold surfaces and therefore is ideal for contact electrification and surface charge density measurements.

The lignin, which we extracted with the acid bomb technique from the nut shell, was used to dope polydimethylsiloxane (PDMS) polymer while preparing the polymer by mixing the prepolymer and the curing agent in 10:1 ratio. The doping concentration of extracted lignin in the polymer mixture was 5% w/w. After mixing thoroughly, the mixture was poured in a Petri dish to achieve a final cured PDMS composite of 0.2 cm height. The mixture was cured at for 4 hrs at 60ºC. Then well-mixed (10:1, base to curing agent) prepolimer of PDMS was poured onto the 0.2 cm thick layer of PDMS-lignin composite to achieve an additional height of 0.3 cm. By this way, only one surface of PDMS pieces was doped by lignin and was prepared for the electrification test. Only one surface, which is doped with lignin, of every PDMS pieces was used for charging experiments.

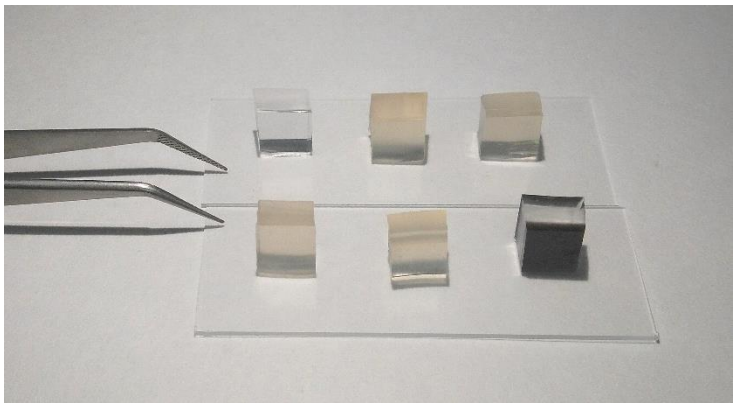

Figure 11. PDMS only, lignin solution doped PDMS pieces with different concentrations and solid lignin doped PDMS pieces.

So far, we mentioned doping lignin inside the polymers in the solid state. We also performed experiments that include doping lignin as a homogeneous solution. Lignin solutions with the concentrations of 0.040, 0,034, 0.028, 0.020, 0.014 mg/ml were prepared by using 1.4 dioxane solvent. These solutions were mixed with elastomers the curing process. Figure 11 shows the PDMS pieces, which are undoped, lignin-solution-doped, and doped with solid lignin. Lignin solutions with the concentrations of 0.040, 0,034, 0.028, 0.020, 0.014 mg/ml, which are shown in Figure 12, were prepared for doping PDMS pieces.

Figure 12. Different lignin solutions with the concentrations of 0.014, 0.020, 0.028, 0.034 and 0.040 mg/ml, increasing from 5 to 1.

2.1.4 Surface Charge Density Measurements

Electrostatic charge on the surface of PDMS can be measured by immersing the pieces in a homemade Faraday cup attached to an electrometer (Keithley 617). Aluminum surface (kitchen foil) was used to contact charge the polymer pieces. Only the lignin doped sides of the PDMS pieces were touched to the Aluminum surface. The electrical charge measured divided by the surface area (charge density) is plotted versus the number of touches. The electrical charge densities of doped and undoped pieces are compared this way. Additionally, we have also performed the charge decay experiments of contact-charged doped and undoped pieces by keeping them immersed in the Faraday cup until the charge decays completely.

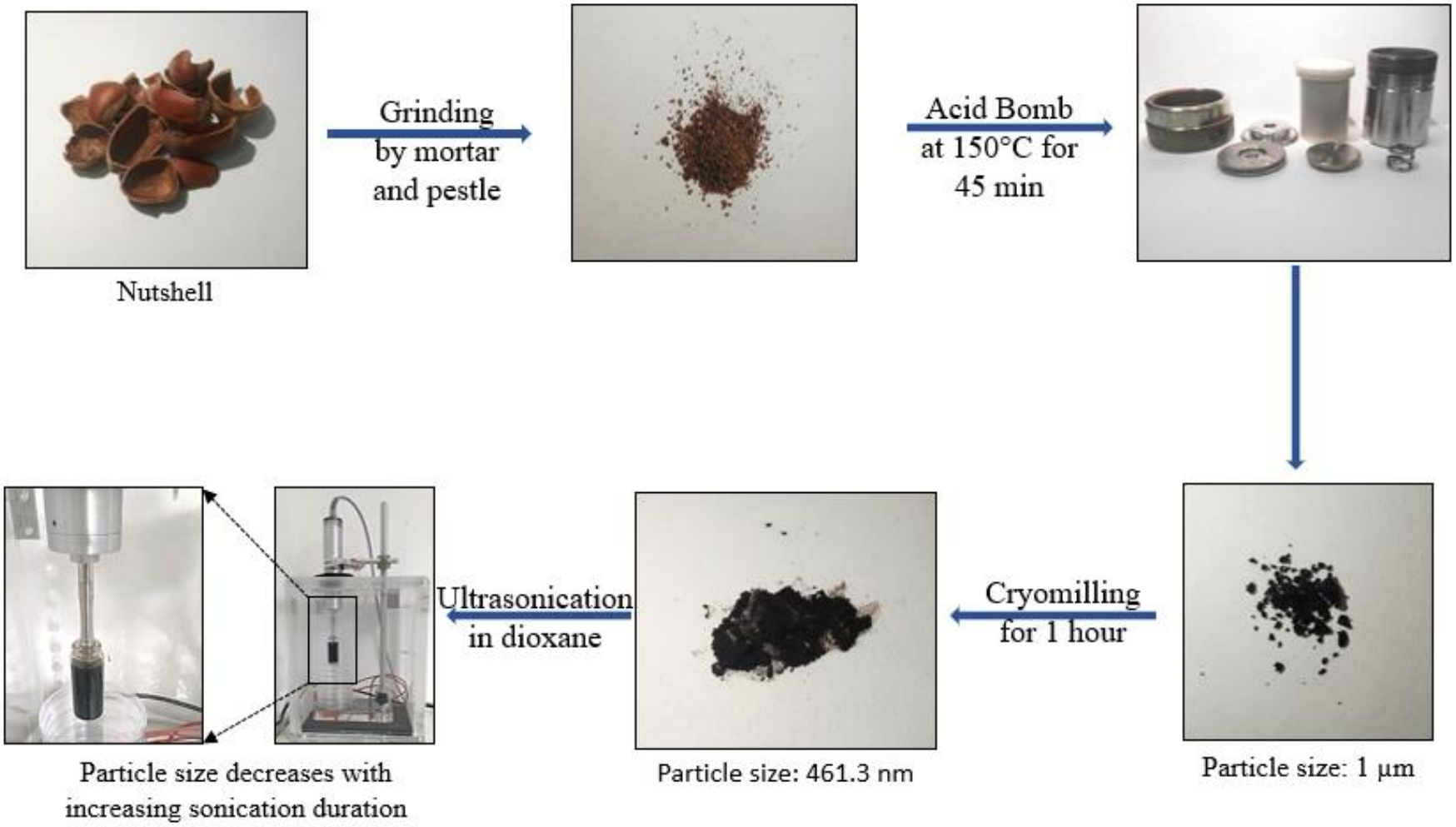

Figure 13. Schematic representation of experiment procedure

2.2 Instrumentation

2.2.1 Cryomill

Cryogenic grinding (cryogrinding) was used as the first step of mechanochemical particle size reduction experiments. Retsch Cryomill, with liquid nitrogen (for attaining cryo temperatures for cooling) from the integrated cooling system, was used for cryogrinding.

2.2.2 Ultrasonication Probe

The second step of mechanochemical particle size reduction process is using ultrasonication horn. Our ultrasonic horn (UP200St Hielscher Ultrasonic Technologies) works at 20 kHz frequency and 200 W power.

2.2.3 Electrometer

Electrostatic charge on the surface of doped and undoped polymers was measured by an electrometer (Kiethley 617) with a Faraday Cup attached.

2.2.4 Zeta Sizer

Particle size distribution analyses of particles were done with Malvern Zeta Sizer instrument. This device allows the determination of the sizes of particles in a range of 5 nm to 50 µm by laser diffraction method. Each measurement was performed three times and average values were collected.

2.2.5 Fourier Transform Infrared Attenuated Total Reflectance (ATR)

Bruker Alpha FTIR Spectrometer was used for the characterization of functional groups in the lignin chemical structure. Spectral width of 4,000–400 cm^{-1}, 64 scans at a resolution of 4 cm^{-1}.

2.2.6 Scanning Electron Microscopy (SEM)

The surface morphology of extracted lignin was imaged with a FEI Quanta 200F model SEM with an accelerating voltage of 15 kV with a spot size of 3.5. Nano and micro lignin particles were analyzed by this imaging method. Also, particles sizes were determined approximately.

2.2.7 ^{31}P NMR Analysis

Lignin samples were derivatized with 70 µl of 2-chloro-4,4,5,5- tetramethyl-1,3,2-dioxaphospholane. 30 mg of the samples were dissolved in a solvent mixture (1.6:1 ratio pyridine/ chloroform). 400 µl of this solvent mixture and 140 µl of a mixture of cholesterol and $Cr(C_5H_7O_2)_3$ with 1:1 ratio was added to the sample. Cholesterol was used as the internal standard, and $Cr(C_5H_7O_2)_3$ was used as the relaxation reagent. The ^{31}P NMR spectra were recorded on a Bruker 400 NMR spectrometer with 6000 scans. The NMR spectra were processed using Bruker-Topspin software.

2.2.8 UV-Vis Spectrometer Analysis

Cary 300 UV-Vis Spectrophotometer was used to measure the absorbance change according to concentration of lignin-1,4 dioxane solutions and identify the specific lignin absorption wavelength, which is 241 nm.

2.2.9 Semiconductor Parameter Analyzer & Probe Stations

Surface resistivity measurements were done by Semiconductor Parameter Analyzer & Probe Stations. Current vs Voltage curves were obtained for lignin doped polymers and undoped polymers. Surface conductivities of samples were measured using a two-probe method, with w = 4.26 mm (width of samples), and the distance between electrodes d = 100 µm. Applied voltage was changed from 0 to 100 V in steps of 10 V and also from 0 to -100 V in steps of 10 V, which gave identical results in terms of conductivity. From the slopes of the I-V curves, the values for surface resistivity were calculated, Rs, according to equation $Rs = (V/I)\cdot(w/d)$.

CHAPTER 3

3 RESULTS & DISCUSSION

3.1 Characterization of Extracted Lignin

3.1.1 FTIR-ATR Spectroscopy Analysis

3.1.1.1 Identification of Functional Groups in Extracted Lignin Samples

The functional groups of the lignin structure have been investigated by FTIR-ATR analyses. IR bands we observed in IR spectra shown in Figure 15 for the extracted lignin sample can be seen in Table 5, with the corresponding peak assignments from the literature (vide infra). On the other hand, Figure 14 shows the FTIR spectrum of extracted lignin from sepale wood by Adamalifo et al [42]. The displayed IR bands of the lignin structure in this spectrum are at the same range with our bands (Figure 15). Peaks at the range of 3400-3500 cm^{-1} are attributed to the characteristic O-H stretching vibrations. The bands at 2990-3000 and the shoulder at 2940-2846 are assigned respectively to the aromatic C-H stretching and C-H stretching in methoxy groups, methyl and methylene groups. The aromatic ring and skeleton vibrations are observed as a band between 1420 and 1620 cm^{-1}. C-H in plane deformation of guaiacyl units which are the characteristic peaks for our lignin type, are at the band of 1270- 1080 cm^{-1}.

Wavenumber (cm^{-1})	Vibrations
3400-3460	O-H stretching
2990-3000	aromatic C-H stretching
2940-2846	C-H stretching in methoxy groups, methyl and methylene groups
1460	aromatic ring vibration
1600, 1514, 1420	aromatic skeleton vibrations
1705	C-O stretching in unconjugating carbonyl/carboxyl groups
1270	guaiacyl ring distortion
1080	deformation in C-O bonds of secondary alcohols and aliphatic ethers
1030	C-H in plane deformation of guaiacyl units
854	Out of plane C-H deformations

Table 5. FTIR vibration frequencies detected in ATR spectrum of acid-extracted lignin (see experimental part) and the corresponding peak assignments from groups [39-41].

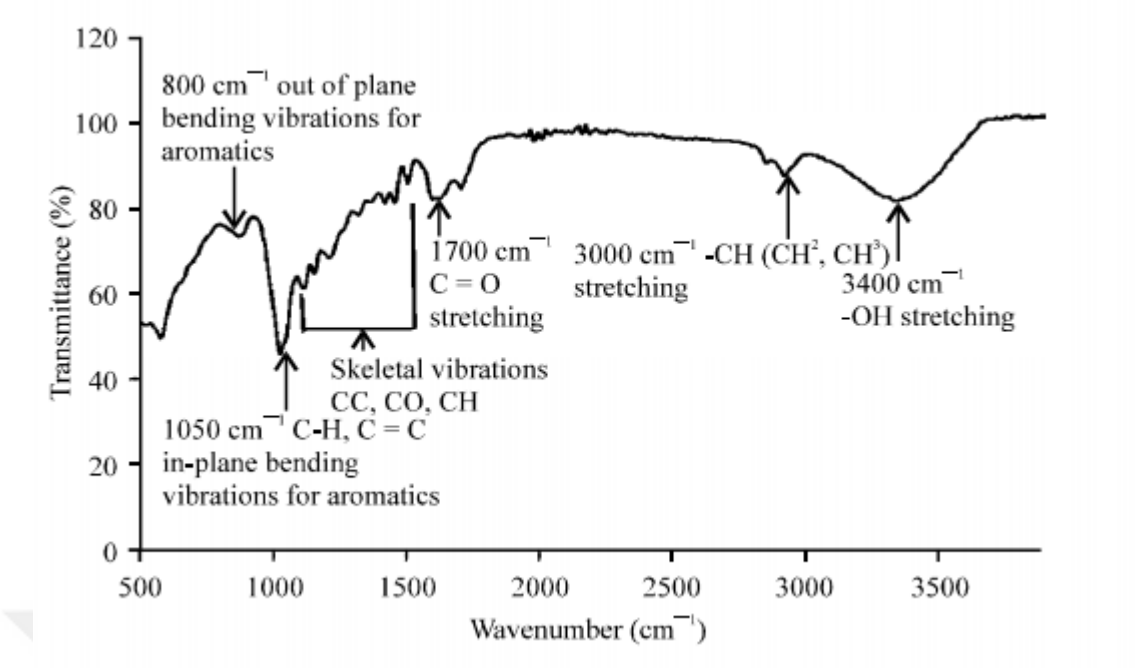

Figure 14. FTIR spectrum of lignin from [42].

3.1.1.2 Structural Changes on Extracted Lignin Samples After Cryomilling

Extracted lignin (30 mg) (see experimental section) was cryomilled for 0, 10, 20, 30, 40, 60 and 120 minutes without solvent and kept under the vacuum for 1 hr. A few mg of the cryomilled sample was subjected to ATR analysis. Figure 15 shows the vibrational changes in IR spectra of the extracted lignin milled for the above-mentioned durations. While the milling duration increases, the intensities of the peaks become sharper and higher. C-O, C-C, C-H skeletal vibrations and C-O stretching between 1200 cm^{-1} and 1600 cm^{-1}, O-H stretching at 3400 cm^{-1}, in-plane-bending vibrations of aromatics at 1030 cm^{-1} can be observed at higher intensities after the cryomilling.

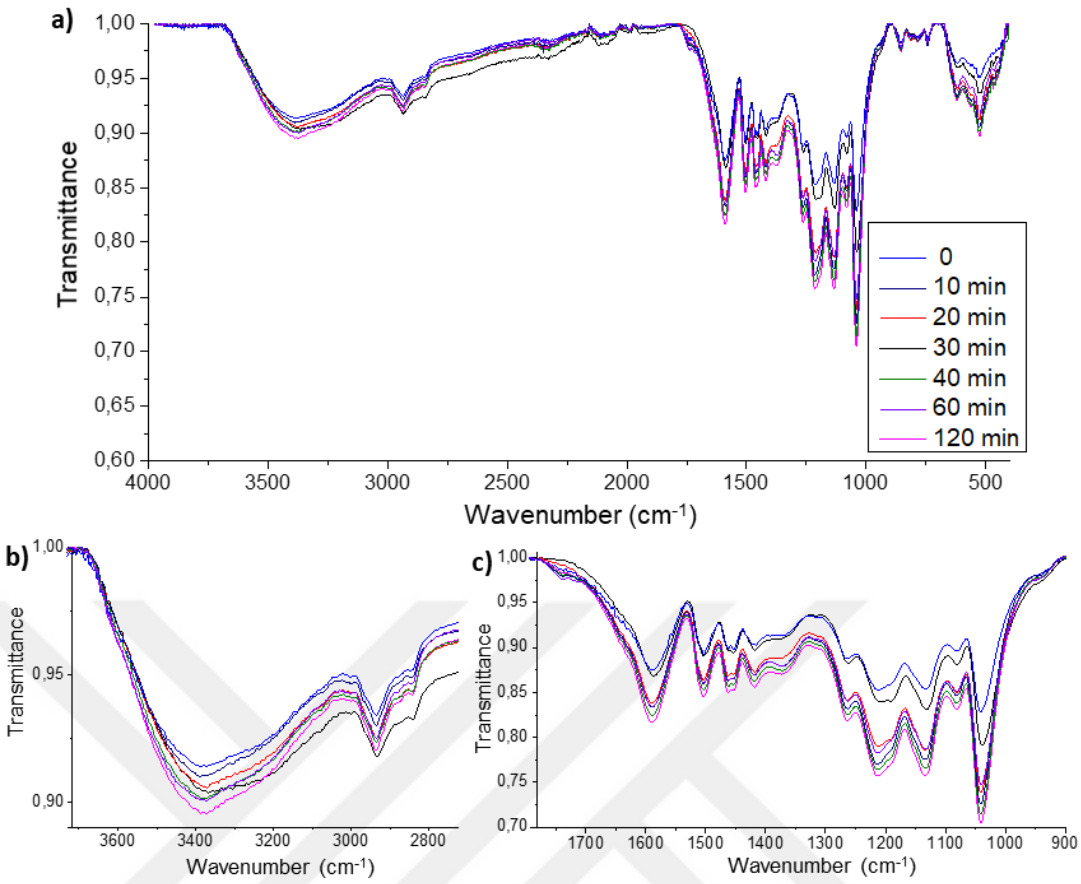

Figure 15. a) FTIR spectra of lignin monitoring increasing cryomilling time. b) Magnified O-H stretching region, c) Aromatic and skeletal vibrations region.

3.1.1.3 Structural Changes of Cryomilled and Ultrasonicated Extracted Lignin Samples

The IR spectra of extracted lignin and nanolignin, which is cryomilled and ultrasonicated to achieve the particle size of ca. 100 nm, were compared in this section. Normalization of a selected peak was done to compare the intensities of the bands emerging from presence of functional groups in the lignin structure by fixing the intensity of the peak at 1500 cm^{-1}. ATR spectrum of the lignin after acid-extraction from the nut shell (red line) and ATR spectrum of this extracted lignin after cryomilling and subsequent ultrasonication (black line) are shown in Figure 16. This FTIR showed increase in hydroxyls, carbonyls, and carboxyl groups. The Spectra of nanolignin shows a significant increase of the intensity of the band at 1705 cm^{-1} which was assigned to carbonyl groups, 1600, 1514, 1424 cm^{-1} belongs to aromatic skeletal vibrations, 3400-3460 cm^{-1} belongs to O-H stretching and 1030 cm^{-1} for C-H in plane deformation of guaiacyl units. Also, intensity of the peak at

1120 cm^{-1} increases. This band was previously represented to condensed aromatic units [39-41].

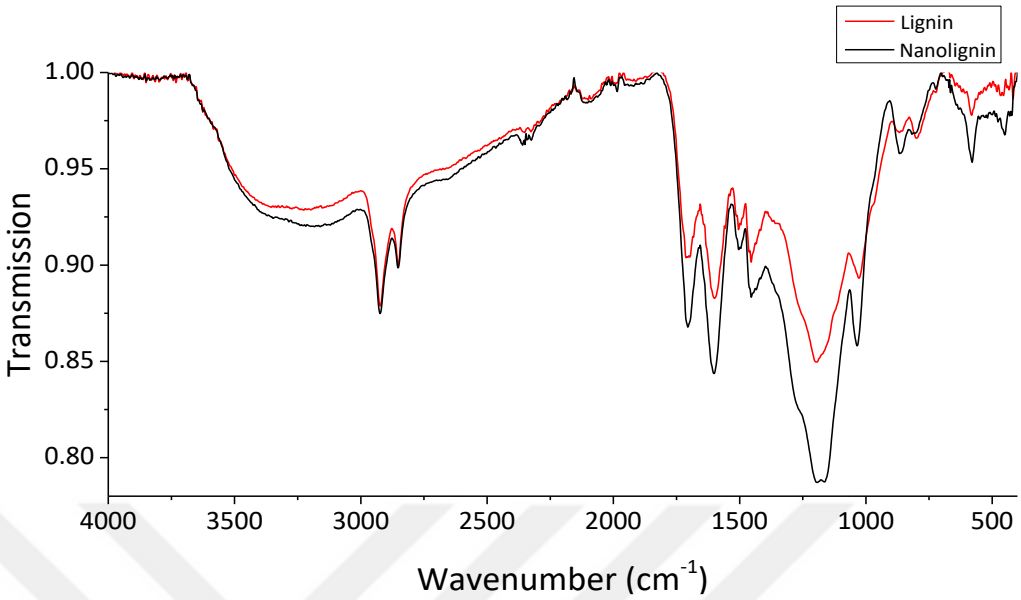

Figure 16. ATR spectrum of the lignin after acid-extraction from the nut shell (red line) and ATR spectrum of this extracted lignin after cryomilling and subsequent ultrasonication ('nanolignin', black line).

3.1.2 Scanning Electron Microscopy (SEM) Analysis

3.1.2.1 Morphological Changes in Mechanochemically Treated Alkali Lignin Samples

To analyze the morphological differences between the lignin particles before and after the mechanochemical treatment, Scanning Electron Microscopy was used. Figure 17 shows the SEM images of alkali lignin before and after mechanochemical treatment. Alkali lignin is produced commercially by alkaline pulping processes of industries to make lignin water-soluble. In Figure 17, images at the top belong to the untreated alkali lignin. Particles have generally round shape and the radius of these particles varies between 30 to 50 µm. On the other hand, images at the bottom shows the particles after cryomilling and ultrasonication processes. Particles seem to have sharp edges on their surfaces due to the mechanical effect and bond-breaking.

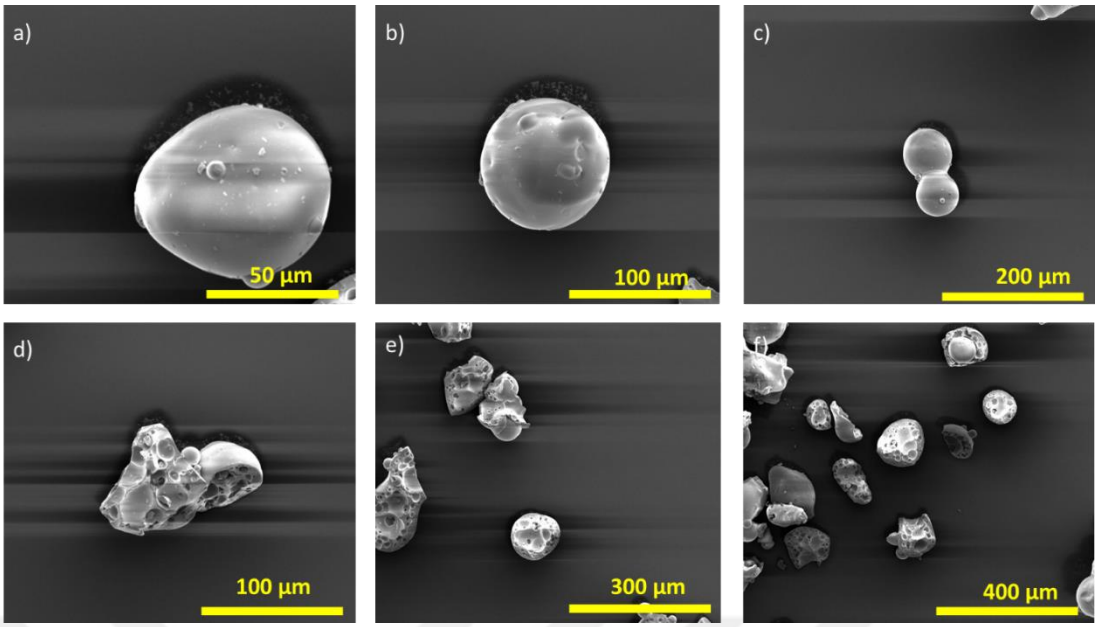

Figure 17. SEM images of alkali lignin particles: a-c) before and d-f) after mechanochemical treatment.

3.1.2.2 Morphological Changes in Mechanochemically Treated Extracted Lignin Samples

After the extraction of lignin from nutshell (see experimental part), lignin sample was dried for SEM analysis. Figure 18 shows SEM images showing the particle size and shapes before and after the mechanical treatment. In the first step of the mechanical treatment, solid extracted lignin was dry milled for 60 min. Then, milled lignin was mixed with 1,4-dioxane to obtain a lignin suspension for ultrasonication treatment. This lignin suspension was sonicated for 60 min. Finally, the solvent was evaporated, and lignin was dried. SEM images (Figure 18), show that particle size decreased from ca. 20 µm to 2 µm after the treatment. Unfortunately, small particles were merged together after the ultrasonication treatment as seen in the bottom row of Figure 18.

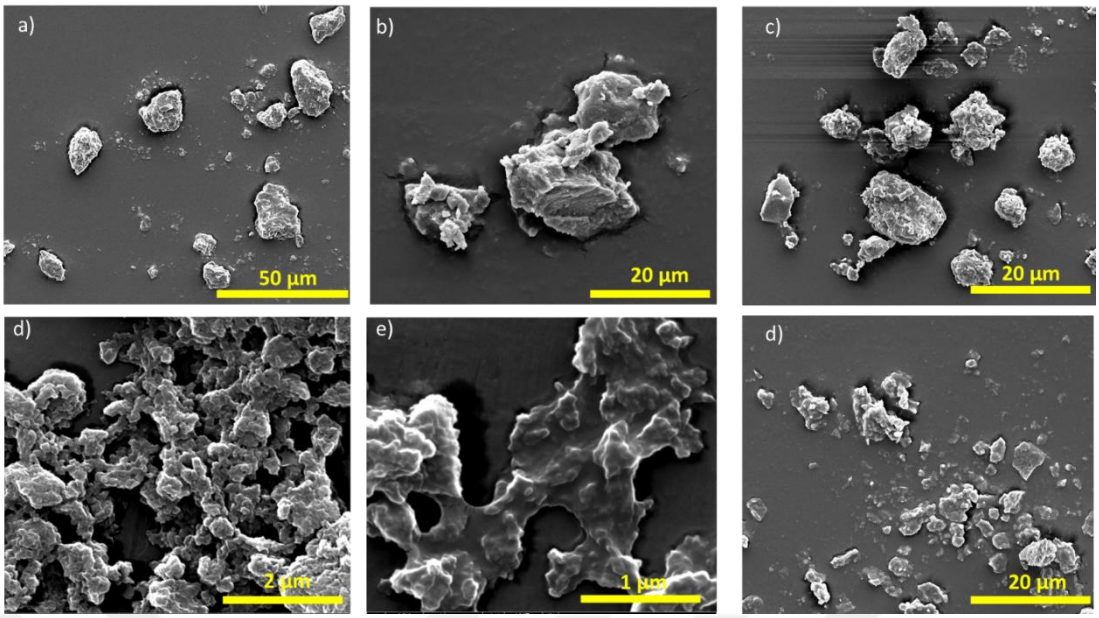

Figure 18. SEM images of extracted lignin particles (see experimental part for acid-extracted lignin): a-c) before and d-f) after mechanochemical treatment involving first cryomilling of 100 mg sample for 60 min, then 30 mg of the cryomilled sample sonicated for 60 min at 20 kHz.

3.1.3 ^{31}P NMR Spectroscopy

^{31}P NMR is a good quantitative method to determine the relative amounts of each type of phenolic OH group existing in lignin. These groups are supposed to take place in the antistatic action. Distribution of O-H groups in the structure of lignin can be analyzed straightforwardly by ^{31}P NMR [17]. The lignin extracted from nutshell was cryomilled for 30, 60 and 120 minutes. Figure 19 shows four ^{31}P NMR spectra which belong to the original sample, 30 min, 60 min and 120 min milled samples. Literature values for ^{31}P NMR shifts from acid extracted lignin and milled lignin are shown in Figure 20. It was observed that, there was an increase in aliphatic, guaiacyl, 'condensed phenolic' OH, carboxylic acid peaks, which are similar to the ones displayed in our ^{31}P NMR spectra for the extracted and milled lignin samples (Figure 19). The relative intensity of aliphatic OH, syringyl OH, and guaiacyl OH increase with increasing milling time [43]. Also, the intensity of the peak for p-hydroxy phenyl units slightly increases with increasing milling time.

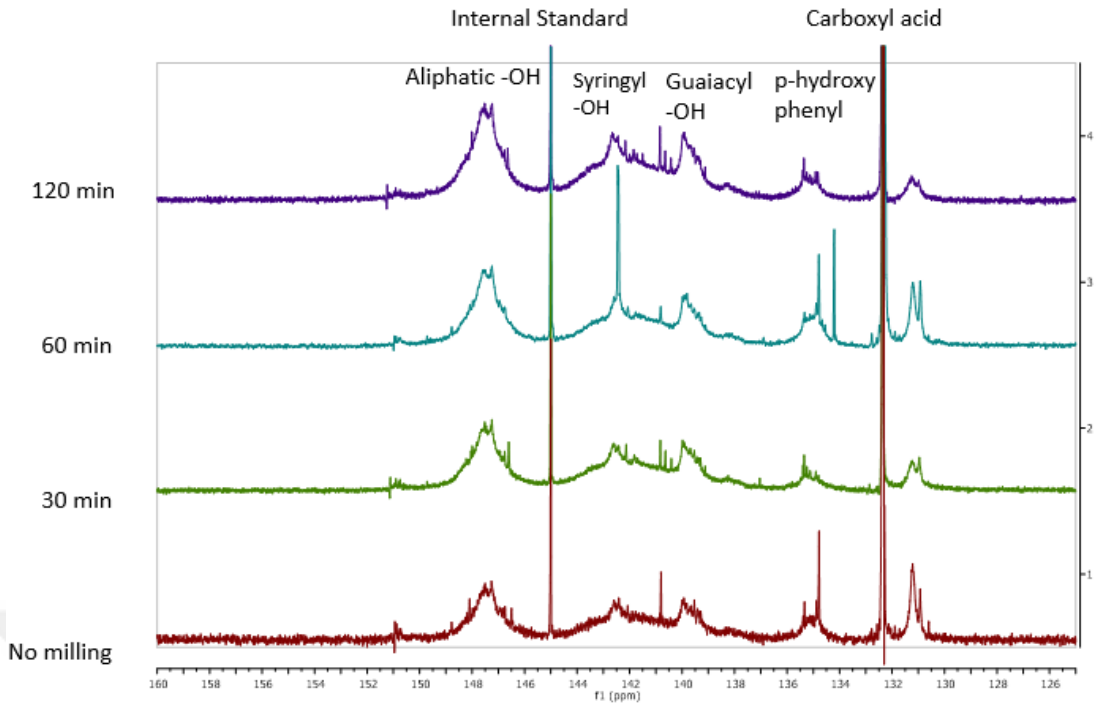

Figure 19. ^{31}P NMR spectra of extracted lignin milled between 0-120 mins.

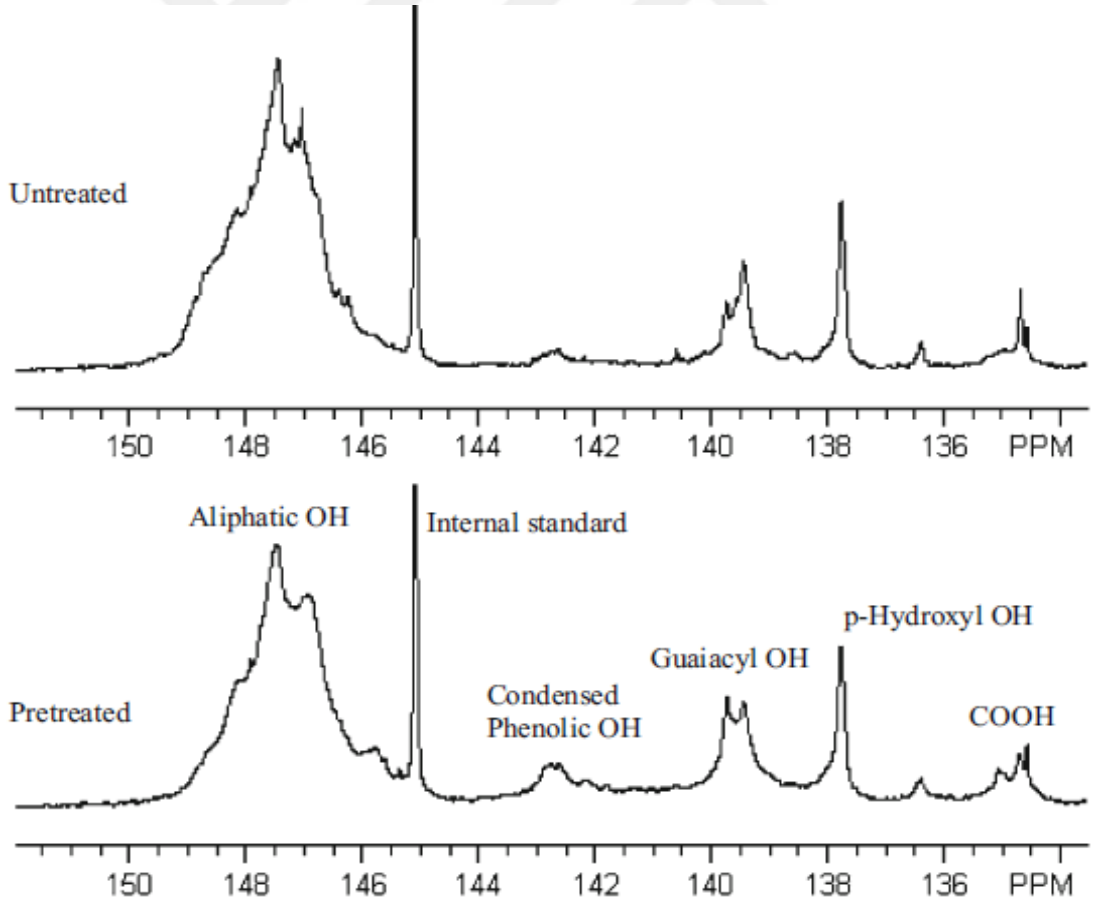

Figure 20. ^{31}P NMR spectra of lignin before and after milling, taken from the literature [44].

3.1.4 UV-VIS Spectrometry

For UV-VIS spectrophotometer measurement, lignin solutions with concentrations of 0.040, 0,034, 0.028, 0.020, 0.014 mg/ml were prepared by dissolving extracted lignin in 15 ml 1,4-Dioxane each. (Figure 21). Before the UV-VIS analysis, samples were diluted 1%.

It is seen that the absorbance values increase with increasing concentration of the solutions. Prior literature shows that lignin species can absorb UV radiation and give peaks in the UV-VIS spectrum, usually in between the wavelength range of 300 to 400 nm, in which range generally chromophore groups absorb. In our measurements, we observe two signals at wavelengths of 280 nm and 240 nm were found. The signal seen at the wavelength of 280 nm is due to the presence of phenolic groups [45]. The signal at the wavelength of 241 nm is due to conjugated double bonds between the carbons, since there are many aromatic groups in the lignin structure [46]. These two bands can be attributed to the high abundance of symmetrical syringyl structures in the hazelnut lignin.

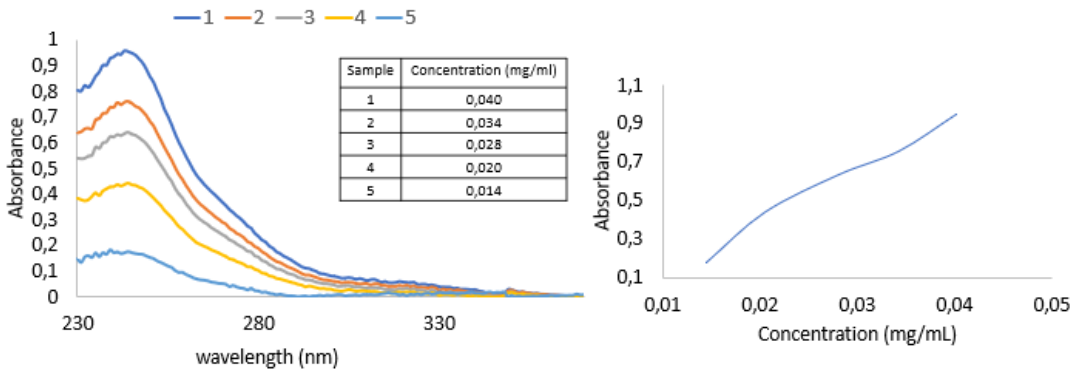

Figure 21. .UV-VIS spectra of acid-extracted lignin (see experimental) solutions at the concentrations of concentrations of 0.040, 0,034, 0.028, 0.020, 0.014 mg/ml. The intensity of peak with absorption maximum at 241 nm is increasing with increasing concentration.

3.2 Particles Size Measurements

3.2.1 Particle Size of Extracted Lignin

At the end of each step, particle size is measured to investigate the effect of milling and ultrasonication on size of the particles and its effect to antistatic property. 40 mg of acid-extracted lignin was dissolved in 10 ml of 1,4 dioxane for each particle size measurement. Figure 22a shows the particle size of untreated extracted lignin, which is found as 1076±2.5 nm. Every measurement was done three times and average values were taken. It is important that the cryomilled and ultrasonicated sample solutions should be measured in max. 1 hour after preparation of samples. Otherwise particles aggregate in solutions and small particle sticks together, which effects the particle size measurements negatively.

3.2.2 Particle Size of Cryomilled Lignin

The extracted lignin was dried under vacuum at 30 ˚C for 24 hours. After that, the 100 mg solid dry lignin sample was milled for 5, 10, 20, 30, 40, 60 and 120 minutes. For every selected minute, approximately 30 mg of the sample was collected and kept under the vacuum at 30˚C for 24 hr. These six samples were dissolved in 10 ml of 1,4 dioxane. The particle sizes of six lignin sample solutions were measured with Zeta Sizer. Figure 22 and Figure 23 show the particle size values. The samples milled for 5, 10, 20, 30, 40, 60 and 120 minutes have the particle sizes of 959.5±2.3, 724.6±2.5, 679.9±3.2, 686.5±2.1, 543.4±2.5, 461.3±2.1 and 436.7±2.5 nm respectively. It can be concluded from the figures that the size of lignin particles decreases with increasing cryomilling duration.

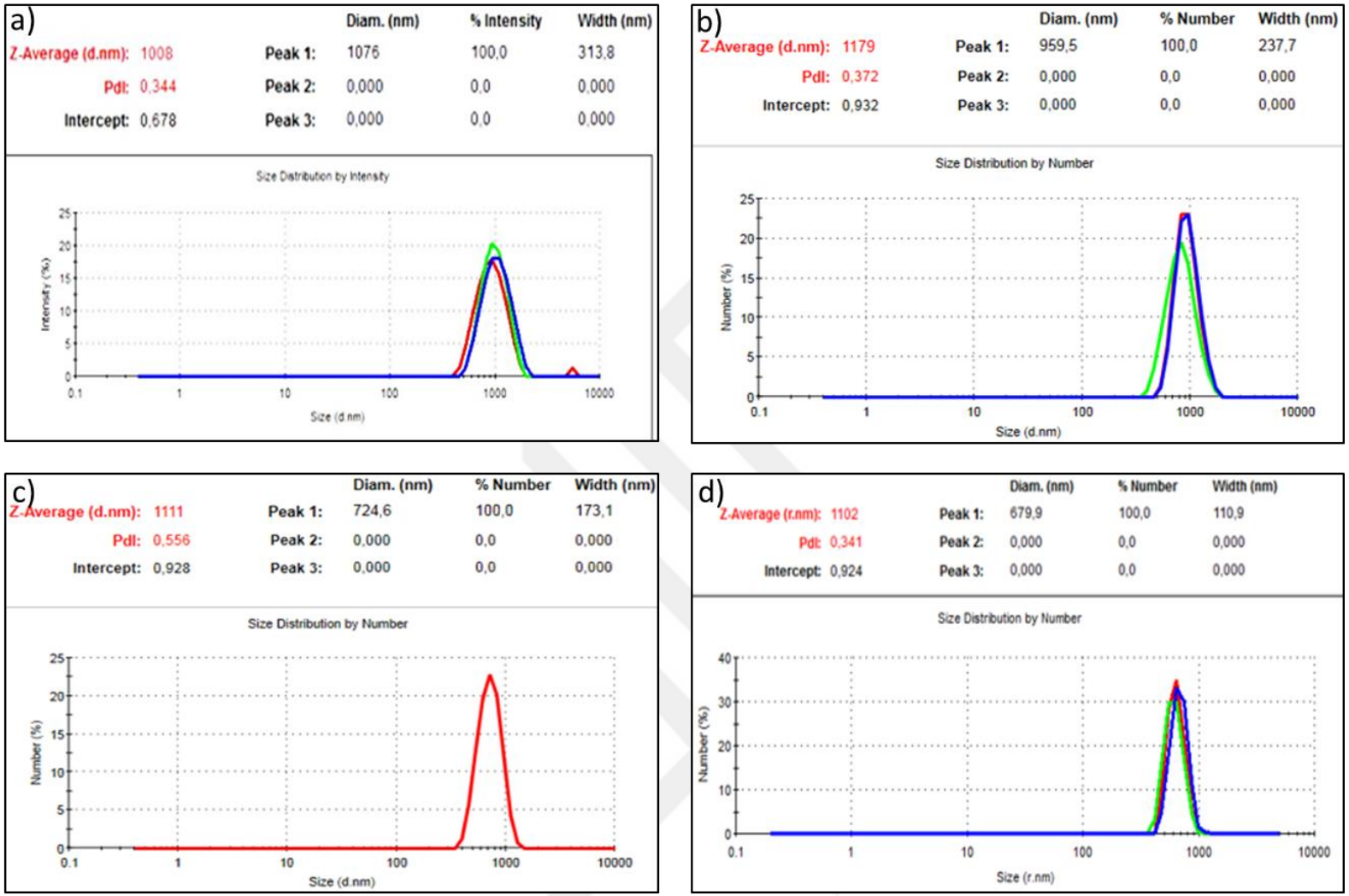

Figure 22. ZetaSizer data for different cryomilling times: a) 0 b) 5 c) 10 and d) 20 mins.

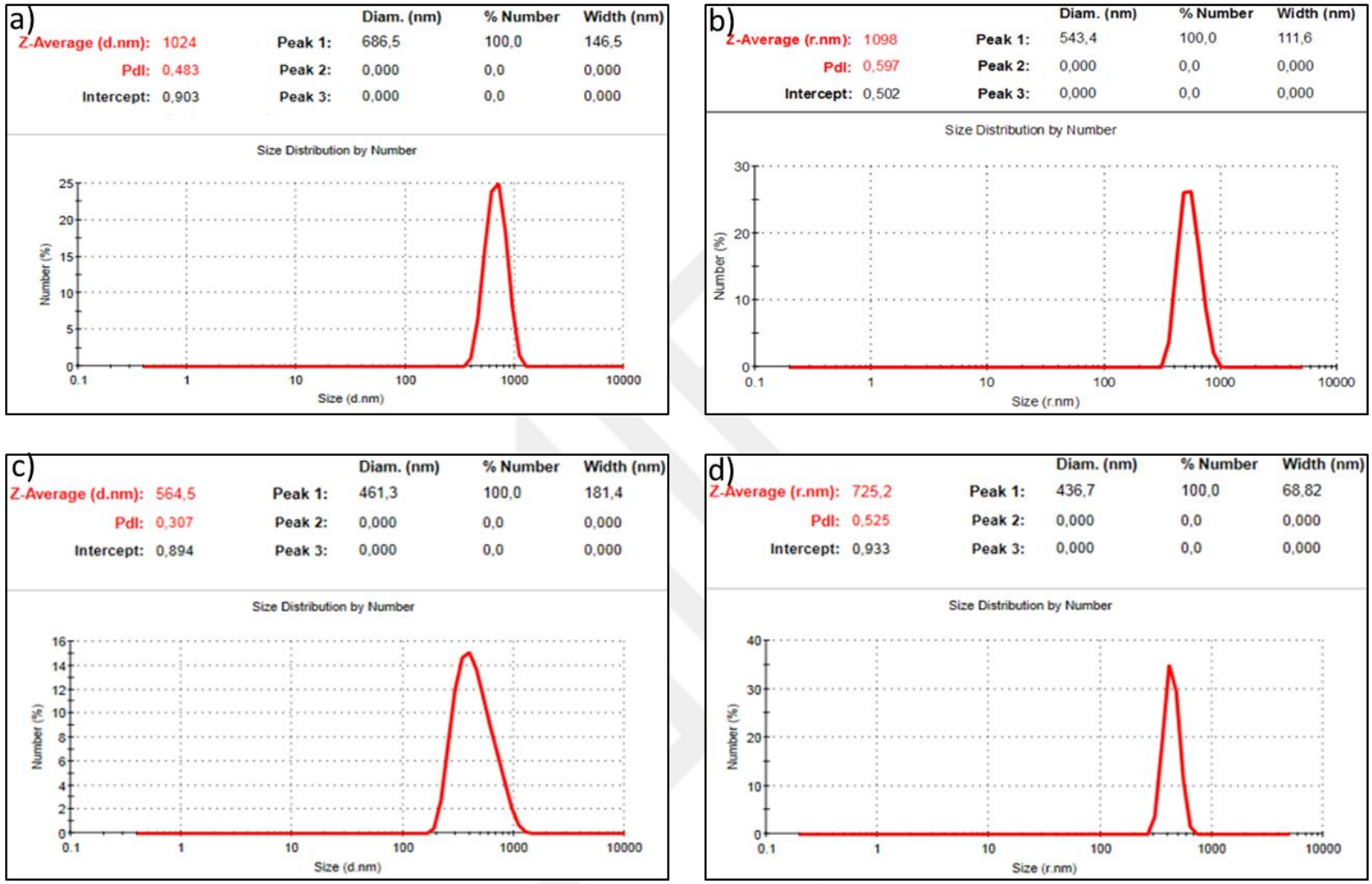

Figure 23. ZetaSizer data for different cryomilling times: a) 30 b) 40 c) 60 and d) 120 mins.

3.2.3 Particle Size of Ultrasonicated Lignin

100 mg of the extracted lignin sample which cryomilled for 120 minutes was used to continue with ultrasonication. During this process, an effective cooling is required. The solution was immersed in an ice water bath to prevent overheating due to the mechanical oscillations, friction and turbulences inside the liquid. Then sample was sonicated for 5, 10, 20, 30, 40, 60 and 120 minutes. Figure 24 and Figure 25 shows that the particles sizes of the particles are 402.7±2.8, 357.6±3.2, 260±2.2, 147.8±3.0, 101.2±2.1, 35,45 ±2.4 and 24.04±3.5 nm respectively. Measurements were performed for three times and average values were taken. Increasing the ultrasonication duration leads to reduction of the particle size of the lignin particles.

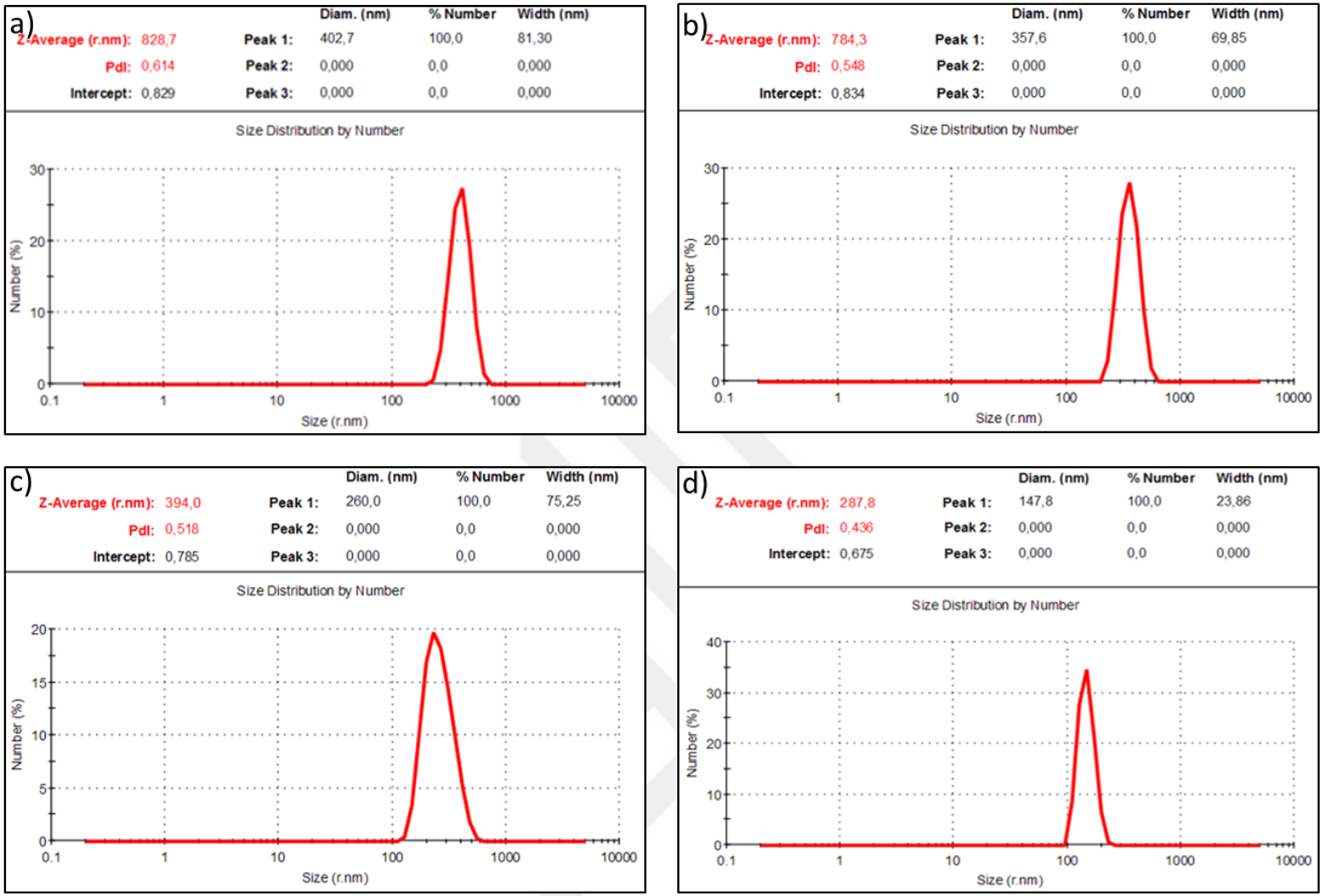

Figure 24. ZetaSizer data for different ultrasonication times: a) 5 b) 10 c) 20 and d) 30 mins.

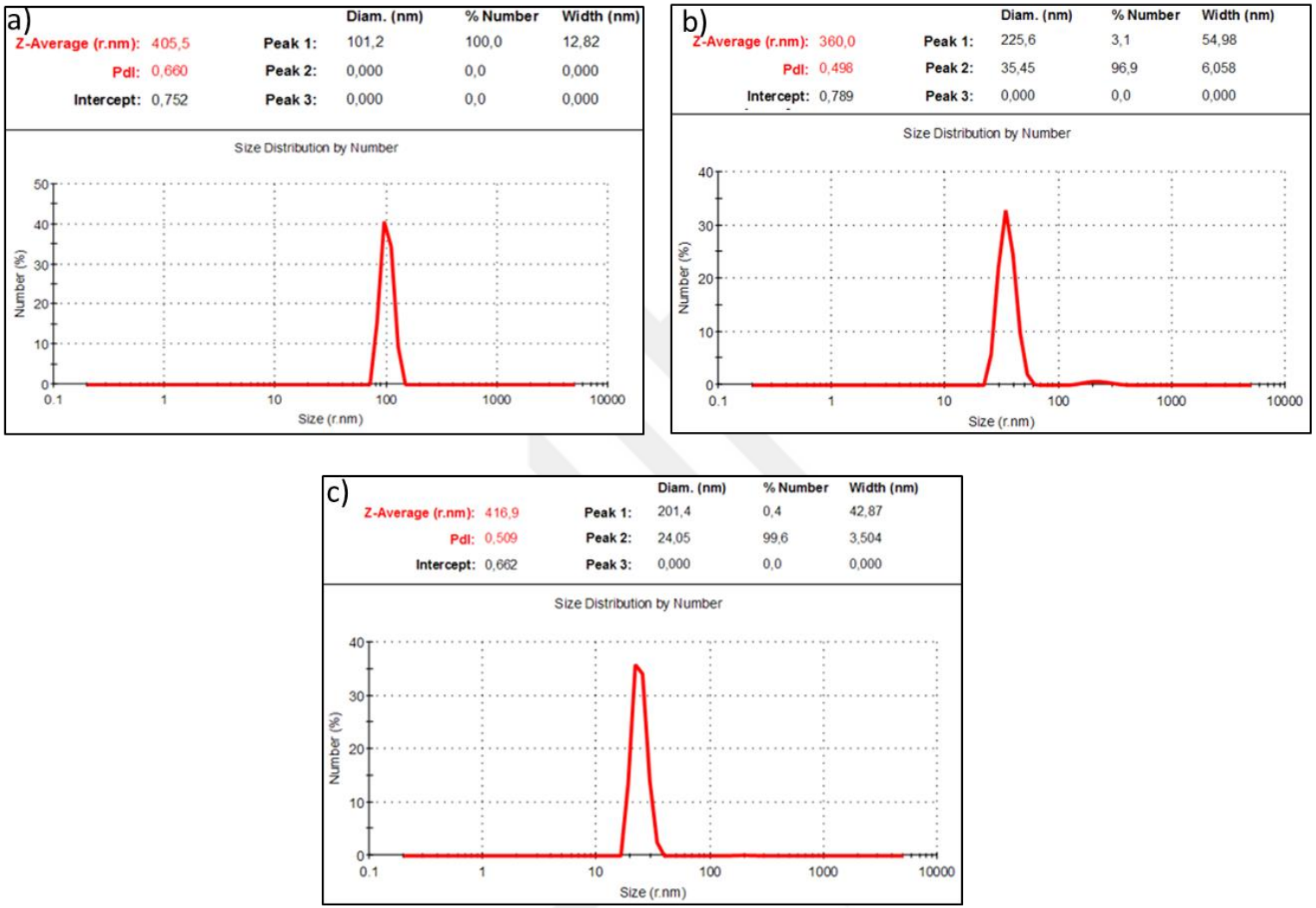

Figure 25. ZetaSizer data for different ultrasonication times: a) 40 b) 60 and c) 120 mins.

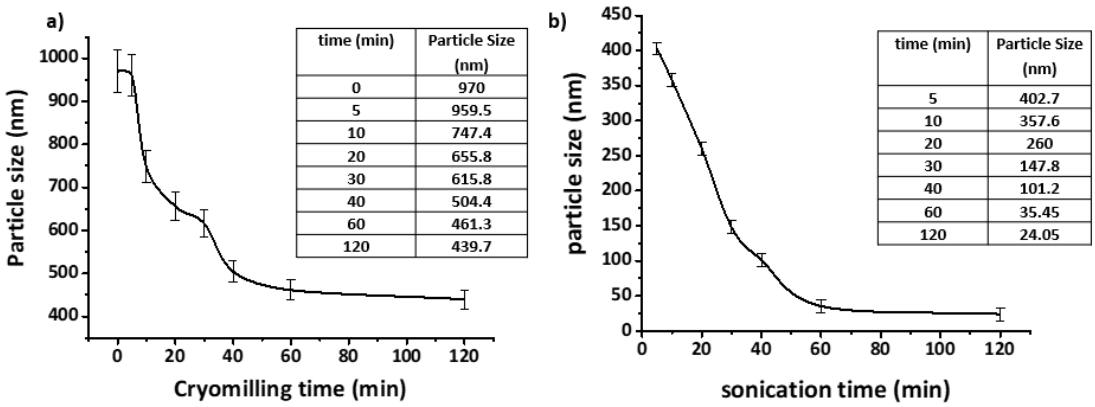

Figure 26. a) Particle size vs cryomilling times and b) Particle size vs ultrasonication times.

3.3 Electrostatic Measurements

A recent study [33] stated that the charge formation on electrified materials is a result of the bond-breakages on the surfaces of the polymeric materials. Both charges (mechanoanion, mechanocation) and the radicals (mechanoradicals) active ends form after the bond breakage. It was also recorded that charges, mechanocations and mechanoanions, are colocalized on the surface with mechanoradicals, which stabilize the charged species. It is possible to destabilize the charges by removing the mechanoradicals by radical scavenger antioxidants, which can be added into the polymer as a doping material. Therefore, radical scavengers can be used as antistatic additives in common polymers.

In this study, we aimed to investigate the radical scavenger property of lignin, which makes lignin a promising antistatic agent candidate. By comparing the electrostatic charge retained on the lignin doped and undoped pieces, and also by monitoring the rate of decay of static charge on these polymers, we assess the extent of antistatic ability upon lignin doping. We also probe surface resistivity to show that 1) the antistatic action of lignin is not due to a conductivity increase but is because of a radical scavenging pathway, 2) the electrical property of the polymer does not change upon doping of lignin.

3.3.1 Contact charging of Nutshell doped PDMS

We initially probe the effect of doping of some ground nutshell to common polymers as explained below to analyze the effect of radical scavenger property of lignin on contact electrification. Doping the nutshell ground is a practical way of having some lignin incorporated within the polymer matrix, before getting into the more complex acid-extraction of the pure lignin. Since nutshell has about 35-45% lignin, and the other major components are cellulose and hemicellulose, we thought doping ground nutshell might show – although somehow minor- antistatic effect. For this purpose nutshell obtained from the west black see region, (60 mg nutshell was milled for 20 minutes by Cryomill) was doped directly inside the prepolymer PDMS as a solid, to have a 5% (w/w) lignin concentration in the final composite. The doped prepolymer PDMS was poured on a Petri dish to reach a thickness of 0.2 cm, cured on a Petri dish. Then undoped PDMS was cured on this sample, to obtain a final thickness of 0.6 cm; this final thickness is then suitable for holding the sample with tweezers. Finally samples were cut with a blade to have (1 cm × 1 cm × 0.6 cm) PDMS pieces. We also separately prepared undoped PDMS pieces with the same final dimensions (Total dimensions of each pieces are 1 cm × 1 cm × 0.6 cm). The PDMS pieces were washed with ethanol (this removes some dirt as well as removes some residual charge that accumulated on the polymer piece during the preparation) and dried before the electrification measurements. After drying, the PDMS pieces were contact-charged against a piece of Aluminum sheet (kitchen Al foil). Following each touch, the charges on the pieces were recorded by immersing the pieces into a homemade Faraday cup connected to the electrometer. Charge versus number of touches plot in Figure 27 shows that the amount of charge on the PDMS pieces doped with ground nutshell is one fourth to one fifth of those accumulated on the undoped PDMS pieces.

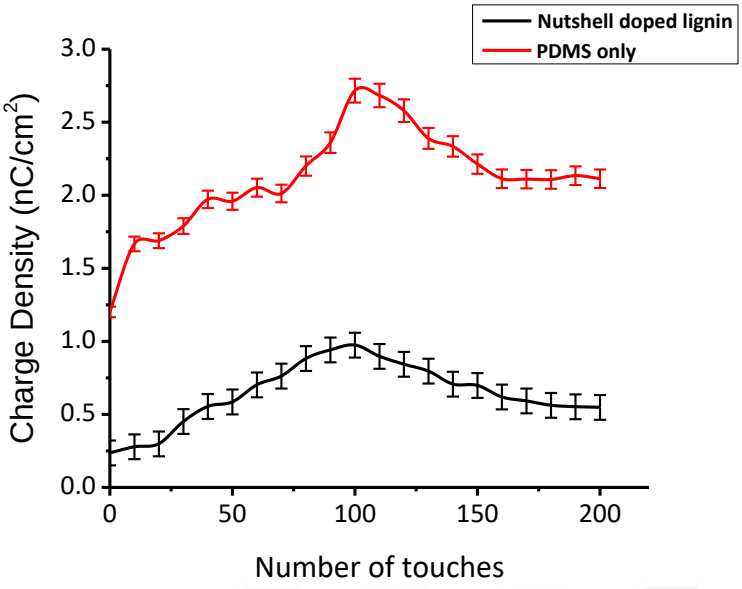

Figure 27: Contact charge accumulated on PDMS pieces doped with ground nutshell and undoped PDMS pieces (1 cm x 1 cm x 0.6 cm) with respect to the number of touches to Al sheet. 60 mg nutshell was milled for 20 minutes by Cryomill and directly doped into PDMS.

3.3.2 Contact Charging of Extracted Lignin and Alkali Lignin Doped PDMS

After the acid extraction of lignin form the nutshell (see experimental part), 30 mg extracted lignin is mixed with the 5 prepolymer PDMS and cured on a Petri dish to have a thickness of 0.2 cm, the height of these pieces were increased to 0.6 cm by curing undoped PDMS polymer on the previously prepared doped PDMS. Similarly, we prepared PDMS samples with commercially available lignin. Commercially available lignin is alkali lignin, which is a salt, so we formed 'protonated' alkali lignin by acidifying an aqueous solution of alkali lignin (pH 10.5) with 1.0 M HCl to achieve a pH of 5. The precipitated lignin is collected, dried and doped into prepolymer PDMS. The rest of the procedure was identical to that for acid-extracted lignin. To serve as controls, undoped PDMS of thickness 0.6 cm was also prepared. All polymers were cut with a blade to obtain sample pieces of 1 cm × 1 cm × 0.6 cm final dimensions and all these PDMS pieces were washed with ethanol and dried before the electrification measurements. After drying, the PDMS pieces were contact-charged against a piece of Aluminum sheet (kitchen Al foil). Following each touch, the charges on the pieces were recorded by immersing the pieces into a

homemade Faraday cup connected to the electrometer. Charge versus number of touches plot in Figure 28 shows that the amount of charges on the PDMS pieces doped with acid-extracted lignin (from nutshell) and 'protonated' alkali lignin are about one fourth to one fifth of those accumulated on the undoped PDMS pieces. It can be concluded that both extracted lignin and acidified lignin can at as an antistatic agent.

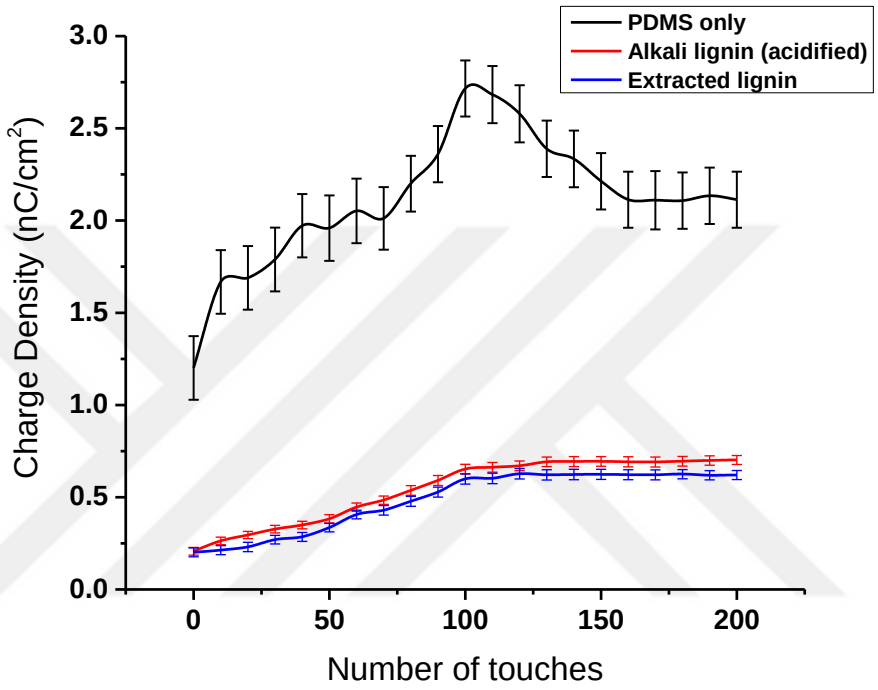

Figure 28. Contact charge accumulated on PDMS pieces doped with 'protonated' alkali lignin and acid-extracted lignin from nutshell, and undoped PDMS pieces (1 cm x 1 cm x 0.6 cm) with respect to the number of touches to Al sheet. 30 mg of lignin with the same particle size (101.2±2.1 nm) was used to dope PDMS. Protonated alkali lignin is prepared as follows: 20 mL solution by addition of 1.0 g alkali lignin was dissolved in 20 mL water, then this solution was titrated with 20 ml HCl solution prepared by dilution of 1.6 ml 37% HCl. The precipitate formed was filtered and dried.

3.3.3 Contact Charging of Cryomilled and Ultrasonicated Lignin Doped PDMS

30 mg of acid-extracted lignin dissolved 10 ml of in 1,4 dioxane with particle sizes of 1000±2.1, 543.4±2.5, 357.6±3.2, 147.8±3.0, 101.2±2.1 and 24.04±3.5 nm, were obtained using cryomilling and ultrasonication (see above). 4 ml of each solution was mixed with prepolymer PDMS and cured at 60ºC for 4 hrs. The solvent evaporated during mixing and curing. Finally, the PDMS pieces (1 cm x 1 cm x 0.6cm) with a uniform lignin distribution were cut. Figure 29 shows the contact charges accumulated on the PDMS samples for each number of touch, from which it is obvious that the maximum charge of the PDMS pieces decreases with decreasing the particle size of lignin particles in the solution. Decay of static charge on these doped polymers are shown in Figure 31.

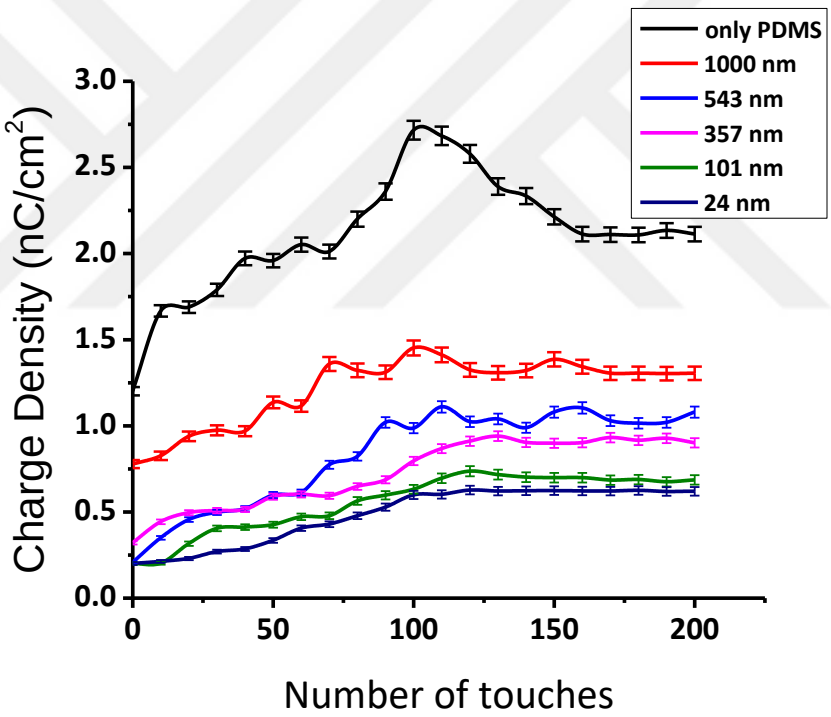

Figure 29. Contact charge accumulated on PDMS pieces doped with lignin solution having 1000±2.1, 543.4±2.5, 357.6±3.2, 147.8±3.0, 101.2±2.1 and 24.04±3.5 nm, lignin particles, and undoped PDMS pieces (1 cm x 1 cm x 0.6 cm) with respect to the number of touches to Al sheet. Charge of lignin solution doped PDMS pieces decreases with decreasing particle size of lignin in the solution.

3.3.4 Contact Charging of Extracted Lignin with Different Concentrations Doped PDMS

0.04 mg/ml, 0.034 mg/ml, 0.028 mg/ml, 0.020 mg/ml, and 0.014 mg/ml lignin solutions in 1,4-dioxane, were prepared. Particle size (101.2±2.1 nm) was same for all samples. The preparation of the polymer pieces were similar to those of the ones described in section 2.1.3. Figure 30 shows that as the concentration of the lignin solution increases, the maximum charge accumulated on the polymer upon touching with Al decreases. Also, decays of static charge of these polymers, which were doped with lignin solutions with the concentrations of 0.04 mg/ml, 0.034 mg/ml, 0.028 mg/ml, 0.020 mg/ml, and 0.014 mg/ml are shown in Figure 31.

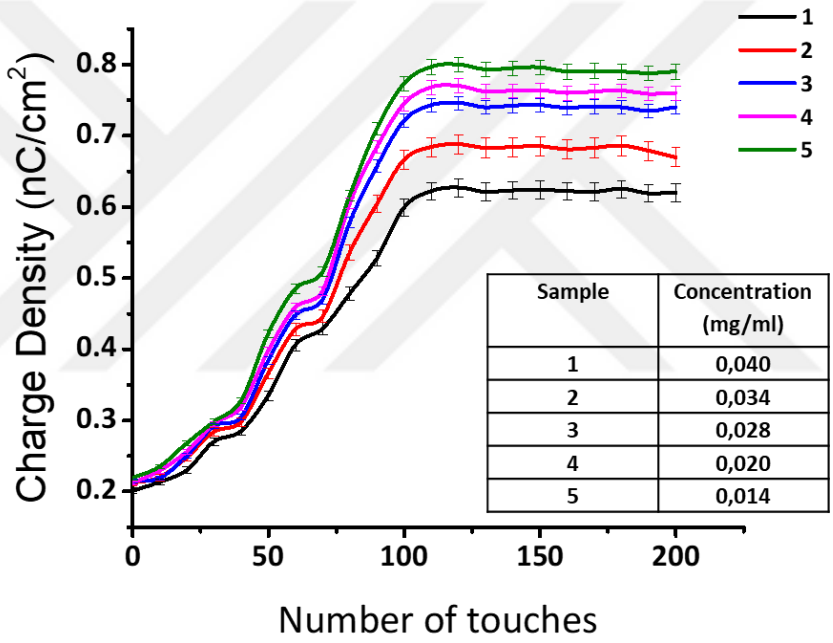

Figure 30. Contact charge accumulated on PDMS pieces doped with lignin solution having 0.04 mg/ml, 0.034 mg/ml, 0.028 mg/ml, 0.020 mg/ml, and 0.014 mg/ml lignin concentrations, and undoped PDMS pieces (1 cm x 1 cm x 0.6 cm) with respect to the number of touches to Al sheet. Particle size = 101.2±2.1 nm. As the concentration of lignin in the solution and thus in the final composite increases, PDMS acquires less charge.

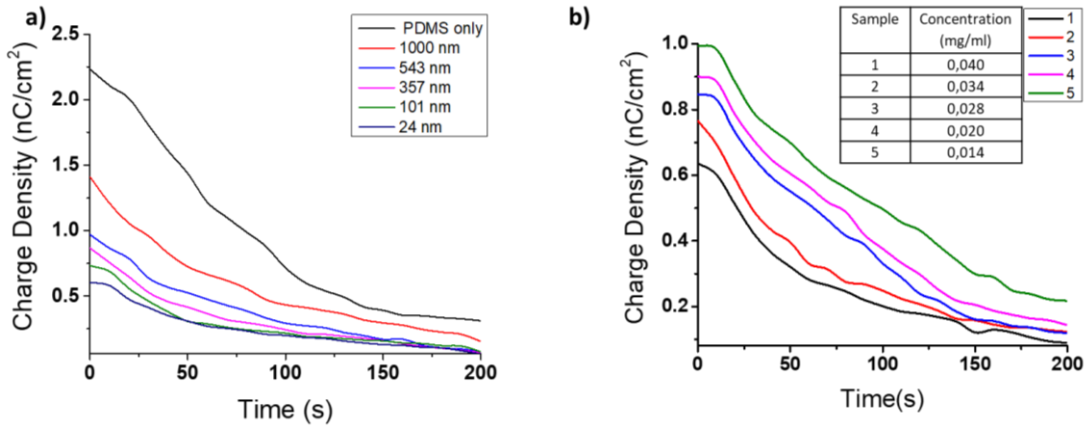

Figure 31. a) Decay curves of lignin solution doped PDMS pieces lignin having particle size of 1000±2.1, 543.4±2.5, 357.6±3.2, 147.8±3.0, 101.2±2.1 and 24.04±3.5 nm. b) Decay curves of lignin solution doped PDMS pieces with lignin concentration of 0.04 mg/ml, 0.034 mg/ml, 0.028 mg/ml, 0.020 mg/ml, and 0.014 mg/ml.

3.3.5 Contact Charging of Extracted Lignin Doped Thermoplastics

So far, we described the antistatic effect of lignin doping in elastomers. To verify that this effect can also be shown for thermoplastics, some examples of thermoplastics, namely, polypropylene, polyethylene and polyvinylchloride were doped with the solid form of the extracted lignin. The contact electrification was again measured according to increasing number of touches on the Al metal surface. PE, PP and PVC sheets were melted in the oven at 170ºC and the extracted lignin was added to these polymers. Mixtures were stirred until a homogeneous distribution of lignin in the polymeric matrix was obtained. PP (2.0 cm × 2.0 cm × 0.2 cm), PE (2.0 cm × 2.0 cm × 0.2 cm) and PVC (2.0 cm × 2.0 cm × 0.2 cm) sheets were prepared by using these molten mixtures. Undoped PP, PE and PVC sheets were also prepared by using the same procedure without doping polymers with lignin. It can be stated from the Figure 33 that undoped PE, PP and PVC have higher contact charging data than the lignin doped PP, PE and PVC for the same number of touches. As a result, we can say that thermoplastics also have the same trend with elastomers. Lignin has a good radical scavenger property to reduce contact charging on the surfaces of both elastomeric and thermoplastic polymers.

To test the antistatic ability of doping polymers with lignin, we used doped PP and undoped PP pieces for contacting them with a piece of nylon for 500 times. Charging

these polymers by contacting with a piece of nylon resulted that when the undoped PP was brought close to small pieces of paper, it attracted them onto its surface. However, when the extracted lignin doped PP polymer piece was brought close to the small pieces of paper, doped polymer had less attracting effect on the pieces of paper (Figure 32).

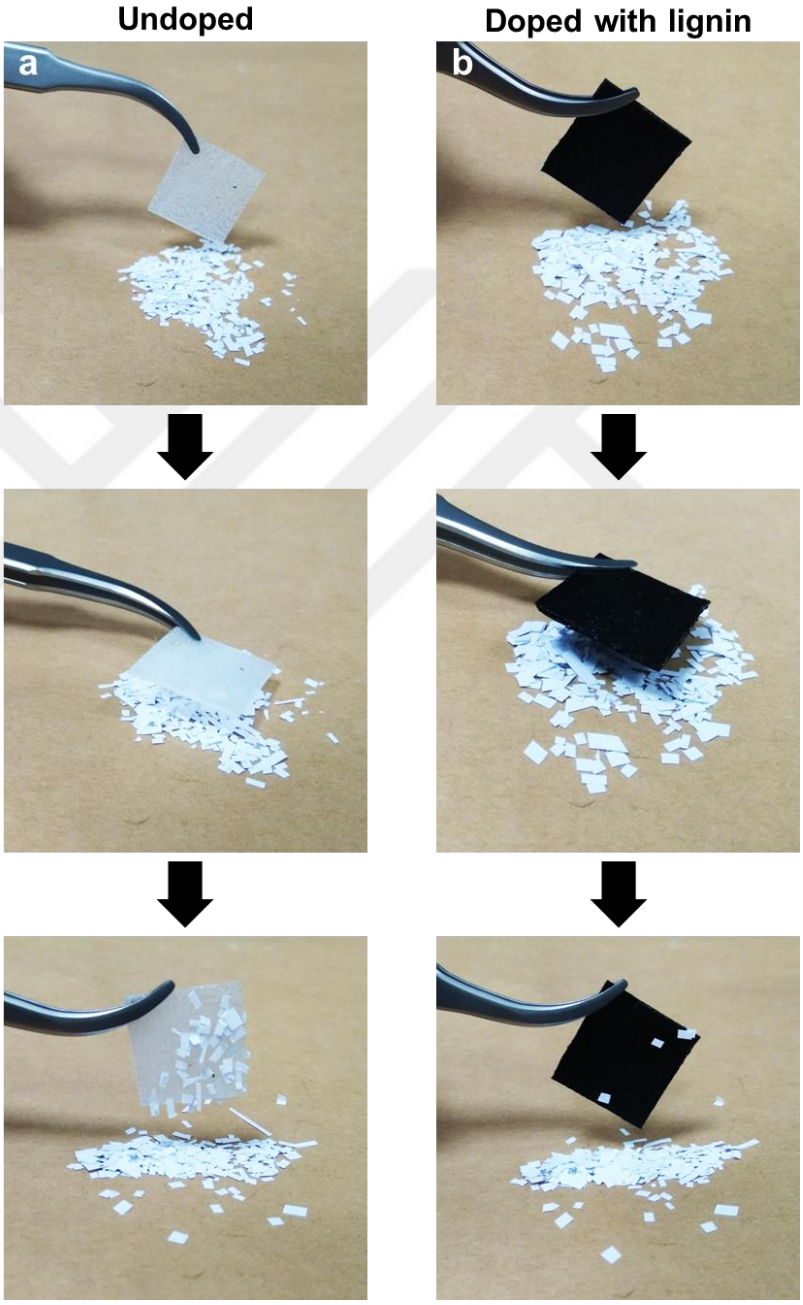

Figure 32. PP doped with lignin reduces charging and adhesion to pieces of paper after contacting with a piece of nylon for 500 times. A piece of a) undoped PP, b) PP doped with lignin was brought close to small pieces of paper.

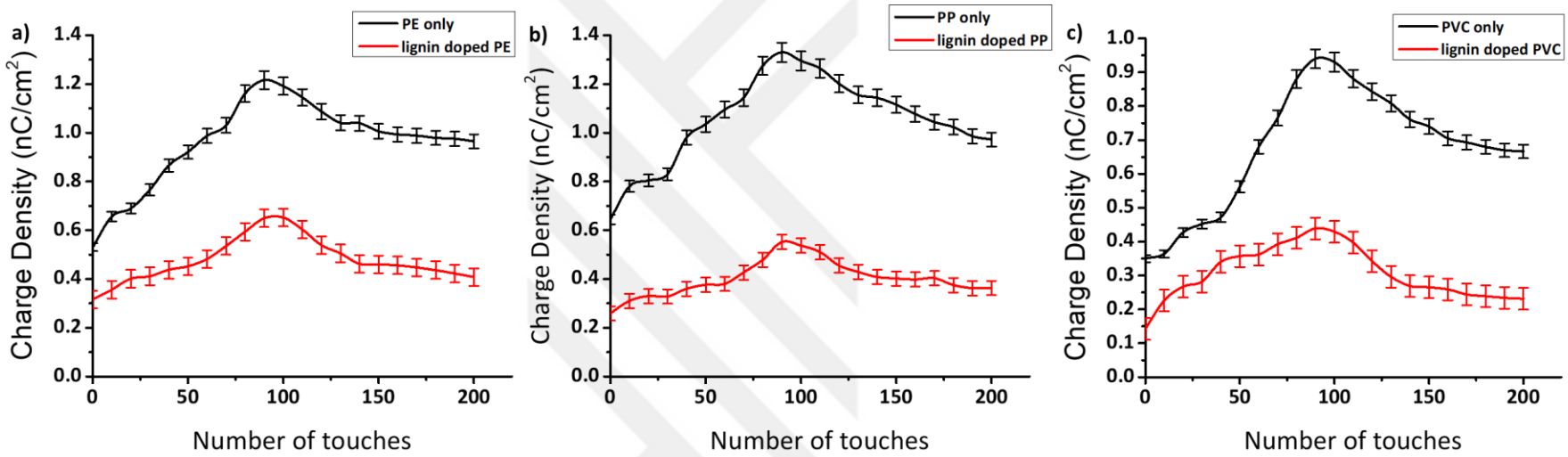

Figure 33. Charging curves of a)lignin doped PP and PP only, b)lignin doped PE and PE only, c)lignin doped PVC and PVC only. Polymers were doped with 60 mg of lignin. The charge of polymers decreases as a result of doping solid lignin into the PDMS pieces.

3.4 Resistivity Measurements

So far we showed that the lignin can be used as an additive in common polymers to reduce the charging on the surface of the polymers. One of the important point is that lignin does not alter the resistivity (or conductivity) of the polymers. This is also important to verify that the antistatic action is because of the radical scavenging but not due to an increase in conductivity upon lignin doping. Therefore, we obtained current versus voltage curves of undoped PP and lignin doped PP (see section 3.3.5 for preparation method) obtained by using a station probe (with w = 20 mm wide samples, and the distance between electrodes d = 100 µm), by which applied voltage was changed from 0 to 100 V in steps of 10 V and also from 0 to -100 V in steps of 10 V. Form the slopes of the I-V curves, the values for surface resistivity, Rs, were calculated, according to equation Rs = (V/I)·(w/d), to be 3.94×10^{-13} and 3.87×10^{-13} ohm/sq for doped and undoped polymers respectively (Figure 34).

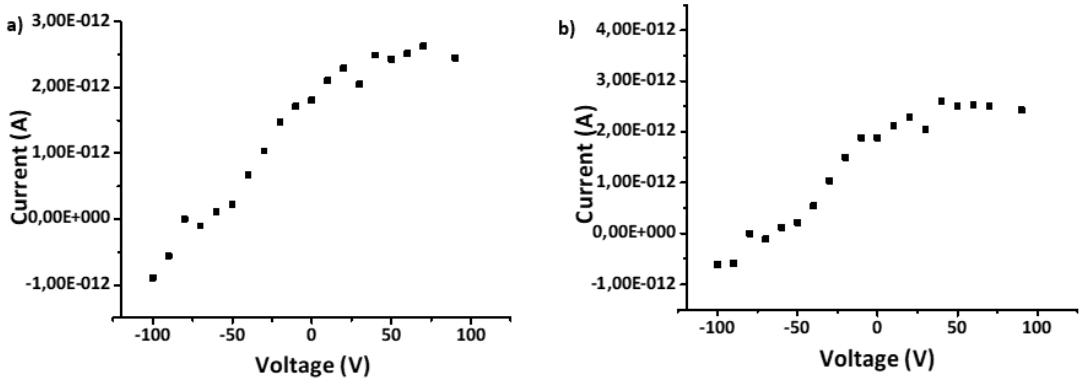

Figure 34. I-V curves of a) lignin doped polypropylene. and b) undoped polypropylene. Samples are 20 mm wide and distance between electrodes is 100 µm.

CHAPTER 4

4 CONCLUSION

With this thesis work, we showed that lignin, which is the second most abundant polymer can be used as an antistatic additive in common polymers, thanks to its phenolic functional groups. These groups can be made more available upon mechanical size reduction (down to 24 nm) of lignin by milling and ultrasonication. The antistatic effect, probed by the surface charge measurements by contact-charging the pieces and immersing them in a Faraday cup connected to an electrometer, can be achieved by doping more lignin into the polymers – as solid or from 1,4 dioxane solutions. Elastomers and thermoplastics can be doped with lignin of 5-10% (w/w), to obtain static charge accumulations of 20-25% of the undoped samples. The polymer composites of lignin with the mentioned doping concentrations was found to be still insulators of electricity, which means that the antistatic action is not due to the increase in conductance – which is the traditional way of eliminating static charges on polymers.

There are many advantages of using lignin for preparing non-charging surfaces. Lignin can be mixed with almost any elastomer and thermoplastic. It is an environmentally friendly polymer, because the molecules that we use are naturally available – in this work we showed that the lignin extracted from nutshell can be used for doping. Lignin is about 100-1000 times less expensive than common molecular radical scavengers and widely available. It is a side product or waste for most of the industries. In the future, we expect a reduction of the usage of unnatural antistatic materials that alter the mechanical/electrical properties of the polymers, more awareness of the green radical scavenging antistatic methods based on the newly enlightened mechanism of contact electrification.

5 BIBLIOGRAPHY

1. Wells, T., Kosa, M., & Ragauskas, A. J. (2013). Polymerization of Kraft lignin via ultrasonication for high-molecular-weight applications. Ultrasonics Sonochemistry, 20(6), 1463-1469.

2. Chen, L., & Jiang, S. (2009). Degradation of Lignin in Aqueous Solution by Ultrasonic Radiation. 2009 3rd International Conference on Bioinformatics and Biomedical Engineering.

3. Crestini, C., & Argyropoulos, D. S. (1997). Structural Analysis of Wheat Straw Lignin by Quantitative31P and 2D NMR Spectroscopy. The Occurrence of Ester Bonds and α-O-4 Substructures. Journal of Agricultural and Food Chemistry, 45(4), 1212-1219.

4. Wool, R. P., & Sun, X. S. (2005). Bio-based polymers and composites. Amsterdam: Elsevier Academic Press.

5. Kharade, A. Y., & Kale, D. D. (1999). Lignin-filled polyolefins. Journal of Applied Polymer Science, 72(10), 1321-1326.

6. McCarthy, J. L., Islam, A., (2000). In Lignin." Historical, Biological, and Materials Perspectives, Vol. 742, American Chemical Society, Washington, DC, pp. 2-99.

7. Nakano, Y., Yamaguchi, M., Endo, H., Rejab, N. A., & Ohtani, M. (2015). NAC-MYB-based transcriptional regulation of secondary cell wall biosynthesis in land plants. Frontiers in Plant Science, vol. 6.

8. Roberts, J. C. (1996). The chemistry of paper. Cambridge: Royal Society of Chemistry, pp. 551-598.

9. Laurichesse, S.; Avérous, L. (2014). Chemical modification of lignins: Towards biobased polymers. Prog. Polym. Sci., vol. 39, pp. 1266–1290. figure extr process

10. Thulluri, C., Pinnamaneni, S. R., Shetty, P. R., & Addepally, U., (2016). “Synthesis of Lignin-Based Nanomaterials/Nanocomposites: Recent Trends and Future Perspectives,” Industrial Biotechnology, vol. 12, pp. 153-160.

11. Nonaka, Y., Tomita, B., and Hatano, Y., (1997). “Synthesis of lignin/epoxy resins in aqueous systems and their properties,” Holzforschung, vol. 51, pp.183—187.

12. LIevonen, M.: Preparation and Characterization of Lignin Nanoparticles, M.Sc. Thesis, Aalto University, School of Chemical Technology, Finland (2014).

13. Calgeris, I., (2010). "Isolation of lignin from nutshell and lignin / starch biodegradable polymers to achieve the "Master's Thesis, Marmara University, Institute of Science and Technology, Istanbul, Turkey.

14. Sjöström E., (1993). "Lignin," in Wood Chemistry, Fundamentals and Applications, E. Sjöström, Ed., San Diego., Academic Press, pp. 71-89.

15. Henriksson, "Lignin," in Pulp and Paper Chemistry and Technology Volume 1. Wood Chemistry G., and Wood Biotechnology, G. G. a. G. H. M. Ek, Ed., Berlin, Walter de Gruyter, 2009, pp. 121-146

16. Feldman, D., Banu, D., Luchian, C., A., Wang, J., (1999b). Epoxy-lignin polyblends: corroletion between polymer interaction and curing temperature. Journal of Applied Polymer Science vol. 42, pp. 1307-1318.

17. Gilca, I. A., Popa, V. I., & Crestini, C. (2015). Obtaining lignin nanoparticles by sonication. Ultrasonics Sonochemistry, 23, 369-375.

18. Feldman, D., Banu, D., Natansohn, A., Wang, J., (1999a). Structure-properties relations of thermally cured epoxy-lignin polyblends. Journal of Applied Polymer Science vol. 42, pp. 1537-1550.

19. Li Y, Mlynar J, Sarkanen S., (1997). “The first 85% kraft lignin-based thermoplastics.

20. Yoshida H., Mörck R., Kringstad Knut P. and Hatake, H., (1987). "Fractionation of kraft lignin by successive extraction with organic solvents, II. Thermal properties of kraft lignin fractions," Holzforschung, vol. 41, p. 171–176.

21. Irvine, G., (1984). "The glass transitions of lignin and hemicellulose and their measurement by differential thermal analysis," Tappi, vol. 67, p. 118–121.

22. Sarkanen K. V. and Ludwig, C. H., (1971). Lignins: occurrence, formation, structure and reactions, New York: Wiley-Interscience.

23. Kinloch, A. J., (1989). “In Rubber Toughened Plastics; Riew, C.K. Ed.,” Advances in Chemistry Series 222, American Chemical Society: Washington, DC, pp 67-91.

24. Rodríguez, J. J., Cordero, T., & Rodríguez-Mirasol, J. (2016). Carbon Materials from Lignin and Their Applications. Production of Biofuels and Chemicals from Lignin Biofuels and Biorefineries, 217-262.

25. Feldman, D., Banu, D., Campanelli, J., Zhu, H., (2001). “Blends of vinylic copolymer with plasticized lignin: Thermal and mechanical properties”, J. Appl. Polym. Sci., 81, pp. 861-874.

26. Demircan, S.F., (2008). Hazelnut shell filled polyethylene composites have mechanical Examination of the properties ", Master Thesis, Marmara University, Institute of Science, Istanbul, Turkey.

27. Yıldırım, A., (2007). "Chopped Hazelnut Shell with Polypropylene Matrix Usability in Composites ", Higher Language Thesis, Marmara University, Institute of Science and Technology, Istanbul, Turkey.

28. Pionteck, J., Wypych, G., (2007). Handbook of Antistatics. Chemical Thecnology.

29. Lowell, J., Rose-Innes, A. (1980). Contact Electrification. Adv. Phys., vol. 29, 947-1023.

30. Raquez, J. M., Habibi, Y., Murariu, M., Dubois, P., (2013). Polylactide (PLA)-based Nanocomposites. Prog. Polym. Sci. vol. 38, 1504-1542.

31. Li, C., Liang, T., Lu, W., Tang, C., Hu, X., Cao, M., & Liang, J. (2004). Improving the antistatic ability of polypropylene fibers by inner antistatic agent filled with carbon nanotubes. Composites Science and Technology, 64(13-14), 2089-2096.

32. J. M. Kolyer, R. Rushworth, and W. E. Anderson, "ESD Control in an Automated Process,"EOS/ESD Symposium Proceedings, EOS-9, 1987, pages 41-50.

33. Baytekin, H. T., Patashinski, A. Z., Branicki, M., Baytekin, B., Soh, S., & Grzybowski, B. A. (2011). The Mosaic of Surface Charge in Contact Electrification. Science, 333(6040), 308-312

34. Baytekin, B., Baytekin, H. T., & Grzybowski, B. A. (2012). What Really Drives Chemical Reactions on Contact Charged Surfaces? Journal of the American Chemical Society, 134(17), 7223-7226.

35. Baytekin, H. T., Baytekin, B., Hermans, T. M., Kowalczyk, B., Grzybowski, B. A. (2013). Control of Surface Charges by Radicals as A Principle of Antistatic Polymers Protecting Electronic Circuitry. Science, vol. 34, 1368-1371.

36. Fang, Y., Gonuguntla, S., & Soh, S. (2017). Universal Nature-Inspired Coatings for Preparing Noncharging Surfaces. ACS Applied Materials & Interfaces, 9(37), 32220-32226.

37. Lacks, D. J.; Sankaran, R. M., (2011). Contact Electrification of Insulating Materials. J. Phys. D: Appl. Phys., 44, 453001.

38. Mehrotra, A., Muzzio, F. J., Shinbrot, T., (2007). Spontaneous Separation of Charged Grains. Phys. Rev. Lett. Vol. 99, 058001.

39. Jiang, C., He, H., Jiang, H., Ma, L., & Jia, D. M. (2013). Nano-lignin filled natural rubber composites: Preparation and characterization. Express Polymer Letters, 7(5), 480-493.

40. Li, Z., & Ge, Y. (2011). Extraction of lignin from sugar cane bagasse and its modification into a high performance dispersant for pesticide formulations. Journal of the Brazilian Chemical Society, 22(10), 1866-1871.

41. Singh, A., Yadav, K., & Sen, A. K. (2012). Sal (Shorea Robusta) Leaves Lignin Epoxidation and Its Use in Epoxy Based Coatings. American Journal of Polymer Science, 2(1), 14-18.

42. Adamafio, N., Kyeremeh, K., Datsomor, A., & Osei-Owusu, J. (2013). Cocoa Pod Ash Pre-treatment of Wawa (Triplochiton scleroxylon) and Sapele (Entandrophragma cylindricum) Sawdust: Fourier Transform Infrared Spectroscopic Characterization of Lignin. Asian Journal of Scientific Research, 6(4), 812-818.

43. Hage, R. E., Brosse, N., Chrusciel, L., Sanchez, C., Sannigrahi, P., & Ragauskas, A. (2009). Characterization of milled wood lignin and ethanol organosolv lignin from miscanthus. Polymer Degradation and Stability, 94(10), 1632-1638.

44. Samuel, R., Pu, Y., Raman, B., & Ragauskas, A. J. (2009). Structural Characterization and Comparison of Switchgrass Ball-milled Lignin Before and After Dilute Acid Pretreatment. Applied Biochemistry and Biotechnology, 162(1), 62-74.

45. Machado, A. E., Furuyama, A. M., Falone, S. Z., Ruggiero, R., Perez, D. D., & Castellan, A. (2000). Photocatalytic degradation of lignin and lignin models, using titanium dioxide: the role of the hydroxyl radical. Chemosphere, 40(1), 115-124.

46. Chatterjee, S., & Saito, T. (2014). Solvent Fractionation of Lignin. ACS Symposium Series Polymer Precursor-Derived Carbon, 153-168.